Molecular Pharmacology Fast Forward. Published on July 15, 2009 as DOI: 10.1124/mol.109.055509
This article has not been copyedited and formatted. The final version may differ from this version.

MOL #55509

Agonist-biased signaling via Proteinase Activated Receptor-2: differential activation of calcium and MAPkinase pathways.

Rithwik Ramachandran, Koichiro Mihara, Maneesh Mathur, Moulay Driss Rochdi, Michel Bouvier, Kathryn DeFea and Morley D Hollenberg*

Department of Physiology and Pharmacology, Faculty of Medicine, University of Calgary, 3330 Hospital Drive NW, Calgary, Alberta T2N 4N1, Canada.

Division of Biomedical Sciences and Cell, Molecular, and Developmental Biology, University of California Riverside, Riverside, CA 92521, USA.

Department of Biochemistry, Institute for Research in Immunology and Cancer, Groupe de Recherche Universitaire sur le Médicament, Université de Montréal, CP 6128 Succursale Centre-Ville, Montréal, Québec H3C 3J7, Canada.

Molecular Pharmacology Fast Forward. Published on July 15, 2009 as DOI: 10.1124/mol.109.055509
This article has not been copyedited and formatted. The final version may differ from this version.

MOL #55509

Running Title: Agonist-biased signaling via PAR_2

Corresponding Author:

Morley D Hollenberg

Department of Pharmacology and Therapeutics and Medicine

University of Calgary,

3330 Hospital Drive NW,

Calgary, AB, T2N4C2

Canada

Molecular Pharmacology Format:

Text pages: 33

Tables: 1

Figures: 11

References: 32

Abstract: 247 words

Introduction: 451 words

Discussion: 1443 words

ABBREVIATIONS:

Amino acids are abbreviated by their one-letter codes: A= alanine, F= Phenylalanine etc.

BRET: Bioluminescence resonance energy transfer

DKO: Double-knockout Beta-arrestin-deficient mouse embryo-derived fibroblasts

EGFR: Epidermal Growth Factor receptor, ErbB1

ERK: Extracellular regulated mitogen-activated kinase or MAPkinase

MAPK: MAP Kinase; P42/44 MAPkinase

MAPkinase: Mitogen-activated protein kinase, or microtubule-associated protein kinase

Molecular Pharmacology Fast Forward. Published on July 15, 2009 as DOI: 10.1124/mol.109.055509
This article has not been copyedited and formatted. The final version may differ from this version.

MEF: Mouse embryo-derived fibroblasts

MMP: matrix metalloproteinase

PAR: Proteinase-activated receptor: PARs 1 to 4.

PAR-AP: PAR-activating peptide

PAR_2 or wt-rPAR_2: wild-type rat proteinase-activated receptor-2, having the trypsin-revealed tethered ligand sequence: SLIGRL---

PAR_2-$A^{37\text{-}38}$: mutated rat PAR_2, with a trypsin-revealed tethered ligand sequence, AAIGRL---

PAR_2-$A^{39\text{-}42}$: mutated rat PAR_2, with a trypsin-revealed tethered ligand sequence, SLAAAA---

PAR_2-$L^{37}S^{38}$: mutated rat PAR_2, with a trypsin-revealed tethered ligand sequence, LSIGRL---

TL: Tethered ligand

Molecular Pharmacology Fast Forward. Published on July 15, 2009 as DOI: 10.1124/mol.109.055509
This article has not been copyedited and formatted. The final version may differ from this version.

ABSTRACT

We evaluated the ability of different trypsin-revealed tethered ligand (TL) sequences of rat proteinase-activated receptor 2 ($rPAR_2$) and the corresponding soluble TL-derived agonist peptides to trigger agonist-biased signaling. To do so, we mutated the proteolytically-revealed TL sequence of $rPAR_2$ and examined the impact on stimulating intracellular calcium transients and MAPkinase. The TL receptor mutants, $rPAR_2$-$L^{37}S^{38}$, $rPAR_2$-A^{37-38} and $rPAR_2$-A^{39-42} were compared with the trypsin-revealed wild-type $rPAR_2$ TL sequence, $S^{37}LIGRL^{42}$---. Upon trypsin activation, all constructs stimulated MAPkinase signaling, but only the wt-$rPAR_2$ and $rPAR_2$-A^{39-42} triggered calcium signaling. Furthermore, the TL-derived synthetic peptide SLAAAA-NH_2 failed to cause PAR_2-mediated calcium signaling, but activated MAPkinase; whereas SLIGRL-NH_2 triggered both calcium and MAPkinase signaling by all receptors. The peptides AAIGRL-NH_2 and LSIGRL-NH_2 triggered neither calcium nor MAPkinase signals. Neither $rPAR_2$-A^{37-38} nor $rPAR_2$-$L^{37}S^{38}$ constructs recruited β-arrestins-1 or -2 in response to trypsin stimulation, whilst both β-arrestins were recruited to these mutants by SLIGRL-NH_2. The lack of trypsin-triggered β-arrestin interactions correlated with impaired trypsin-activated TL-mutant receptor internalization. Trypsin-stimulated MAPkinase activation by the TL-mutated receptors was not blocked by inhibitors of $G\alpha_i$ (pertussis toxin), $G\alpha q$ (GP2A), Src kinase (PP1) or the EGF receptor (AG1478), but was inhibited by the Rho-kinase inhibition (Y27362). The data indicate that the proteolytically-revealed TL sequence(s) and the mode of its presentation to the receptor (tethered vs soluble) can confer biased signaling by PAR_2, its arrestin recruitment and its internalization. Thus PAR_2 can signal to multiple pathways that are differentially triggered by distinct proteinase-revealed TLs or by synthetic signal-selective activating peptides.

Molecular Pharmacology Fast Forward. Published on July 15, 2009 as DOI: 10.1124/mol.109.055509
This article has not been copyedited and formatted. The final version may differ from this version.

INTRODUCTION

Proteinase-activated receptors (PARs) are unique members of the G-protein-coupled superfamily of receptors (GPCRs), modeled as seven transmembrane domain cell surface receptors that mediate diverse signaling events in response to proteolytic exposure of an N-terminal tethered ligand (TL) sequence. PAR_2, the second member of this family to be cloned (Bohm et al., 1996; Nystedt et al., 1994) is a serine proteinase-activated class A GPCR, with an unusual 'tethered ligand' (TL) receptor activation mechanism (Coughlin, 2000; Ramachandran & Hollenberg, 2008). Proteolytic cleavage by serine proteinases, prototypically trypsin for PAR_2, reveals a sequence within the receptor N-terminus (S^{37}LIGRLDTP^{45}--- in rodent PAR_2), that then acts as a tethered receptor-activating ligand (TL), presumably by interacting with other cell surface receptor domains. Interestingly, PAR_2 is also triggered by soluble synthetic receptor-activating peptides (PAR_2-APs) with sequences corresponding to that of the proteolytically revealed TL (e.g. SLIGRL-NH_2).

Our previous work aimed at identifying PAR_2 TL amino acids responsible for signaling has delineated residues within the trypsin-revealed receptor TL sequence which are critical for triggering elevations in intracellular calcium (Al-Ani et al., 2004). The first two amino acids of the trypsin-revealed TL ($S^{37}L^{38}$) were found to be important, such that a revealed rat PAR_2 mutated TL sequence, SLAAAA---, was able to stimulate increases in intracellular calcium, whereas the revealed mutated TL sequences, LSIGRL--- or AAIGRL--- were not. Further, we showed that, whereas the sequence SLAAAA--- could activate calcium signaling as a tethered ligand, the corresponding soluble synthetic peptide, SLAAAA-NH_2, was unable to do so. These data pointed to differences in signal trafficking by PAR_2, depending on whether it is activated by its own proteolytically revealed TL or by an analogous synthetic peptide. For many other G-protein-coupled receptors, such as those for angiotensin II, dopamine, serotonin and adrenergic ligands, it is now accepted that there can be differential signaling, depending on the activating ligand.

Molecular Pharmacology Fast Forward. Published on July 15, 2009 as DOI: 10.1124/mol.109.055509
This article has not been copyedited and formatted. The final version may differ from this version.

This agonist-dependent differential signaling has been termed 'agonist-biased signaling' or 'functional selectivity' (Galandrin et al., 2007; Kenakin, 2007; Urban et al., 2007; Wei et al., 2003). We therefore hypothesized that in a unique way, the trypsin-revealed PAR_2 TL might, depending on its sequence, exhibit functional selectivity, so as to target signaling to distinct responses (e.g. calcium versus MAPkinase). To test this hypothesis, we examined rat PAR_2 receptor mutants with different revealed TL sequences (described above) for their ability to signal (or not) by (1) either elevating intracellular calcium or activating ERK/p42/44 MAPkinase (or both), (2) recruiting β-arrestins -1 and -2 and (3) promoting endocytosis. These three responses were monitored upon activating the wild-type and TL-mutated receptors both by a proteinase (trypsin) and by a series of soluble synthetic PAR-AP analogues with amino acid sequences corresponding to those of the N-terminal proteinase-revealed wild-type or mutated tethered ligands.

Molecular Pharmacology Fast Forward. Published on July 15, 2009 as DOI: 10.1124/mol.109.055509
This article has not been copyedited and formatted. The final version may differ from this version.

MATERIALS AND METHODS

Chemicals and other reagents:

Enzyme inhibitors (PP1 for Src; Y27362 and H1152 for Rho kinase; Doxycycline for metalloproteinases; PD153035/AG1478 for the EGF receptor kinase) were obtained from Calbiochem (La Jolla, CA). The Gαq inhibitor, GP2A (used at a concentration of 10 μM) was from Tocris Bioscience, Ellisville, MO, USA. Culture medium (Dulbecco's modified Eagles Essential Medium: DMEM) and fetal bovine serum (FBS) was from Gibco/Invitrogen Life Sciences (Burlington, ON). Pertussis toxin and calcium ionophore A23187 were from Sigma (St. Louis, MO). Porcine trypsin (catalog number T-7418; approx. 14,900 units/mg) was also obtained from Sigma (St. Louis, MO). A maximum specific activity of 20,000 units/mg was used to calculate the approximate molar concentration of trypsin in the incubation medium (1 unit/ml ≅ 2 nM). All PAR-activating peptides and analogues were synthesized as C-terminal amidated products by the Faculty of Medicine Peptide Synthesis facility at the University of Calgary (Peplab@ucalgary.ca) with purity verified by amino acid analysis and mass spectral analysis.

Expression Vectors:

The plasmid encoding the rat PAR_2 receptor (wt-rPAR_2) and the tethered ligand mutated rat PAR_2 receptor variants LSIGRL (rPAR_2-$L^{37}S^{38}$) or AAIGRL (rPAR_2-A^{37-38}) (Table 1) were constructed as described previously (Al-Ani et al., 2004). The YFP tagged variants for all the contructs were generated by ligating the PAR genes into the pEYFP-N1 vector (Clonetech, Mountain View, CA). Plasmids encoding the Gα12 and Gα13 genes in the pCDNA3.1+ vector were obtained from the University of Missouri S&T cDNA resource centre (Rolla, MO). The sequences for all constructs were confirmed by sequencing.

Molecular Pharmacology Fast Forward. Published on July 15, 2009 as DOI: 10.1124/mol.109.055509
This article has not been copyedited and formatted. The final version may differ from this version.

Cell lines and transfection:

KNRK or HEK-293 cells were routinely cultured as outlined previously and passaged without the use of trypsin using an isotonic EDTA-containing dissociation buffer (Al-Ani et al., 2004; Kawabata et al., 1999) in DMEM supplemented with 10% FBS, 1% sodium pyruvate and 1% antibiotic antimycotic solution. The KNRK cells do not express functional PAR_2, as do the HEK-293 cells, and were thus used to generate the permanent PAR_2-expressing cell lines (Table 1) for an evaluation of calcium signaling and MAPkinase activation, in keeping with previous work (Al-Ani et al., 2004). The studies of transiently transfected cells (BRET and internalization) were done with the HEK-293 cells because of their greater transfection efficiency compared with the KNRK cells. Mouse embryonic fibroblasts wild type (MEF WT) and β-arrestin double knockout (MEF βarrDKO), were a gift generously provided by Dr. Robert Lefkowitz (Duke University, Durham NC USA) and were routinely cultured as above, except that cells were passaged by trypsin dissociation, followed by repeated feeding with trypsin-free growth medium. Transfections were performed on cells that were approximately 80% confluent with lipofectamine (Invitrogen, Burlington, ON) or Fugene6 (Roche, Laval, QC). MEF cells were transfected by the calcium phosphate method as described previously (Chen and Okayama, 1987). KNRK rat kidney epithelial cell lines stably expressing equivalent levels of wild-type or the TL-mutant $rPAR_2$ were selected by quantifying cell surface receptor expression levels with flow cytometry using the B5 PAR_2 selective antibody as described previously (Al-Ani et al., 2004). In order to test Gα12 and Gα13 involvement in $rPAR_2$ signaling, KNRK cells stably expressing wt-$rPAR_2$, $rPAR_2$-$L^{37}S^{38}$ or $rPAR_2$-$^{A37\text{-}38}$, were transiently transfected with plasmids encoding the Gα12 and the Gα13 genes for 48 hours prior to use in experiments studying cell signaling.

Molecular Pharmacology Fast Forward. Published on July 15, 2009 as DOI: 10.1124/mol.109.055509
This article has not been copyedited and formatted. The final version may differ from this version.

Calcium Signaling:

Calcium signaling responses were monitored as described previously (Kawabata et al., 1999). In brief, cells were grown to 80% confluence, lifted in enzyme free cell dissociation buffer (Gibco) and were incubated with 5μM Fluo3-AM (Invitrogen) for 30 min at room temperature in the presence of sulfinpyrazone (0.25 mM). Fluo3 loaded cells, washed free of extracellular calcium indicator, were placed in stirred plastic cuvettes (VWR) and agonist stimulated calcium mobilization and concomitant increases in fluorescence were monitored with an Aminco Bowan series II fluorimeter using the AB2 software (Thermo Fisher Scientific, Nepean, ON). Calcium signals monitored using an excitation wavelength of 480 nm and an emission wavelength recorded at 530 nm were expressed as a percentage of the emission fluorescence caused by 2μM calcium ionophore A23187 (E_{530}, % A23187) (Kawabata et al., 1999).

Western Blotting:

KNRK cells transfected with wt-rPAR$_2$, rPAR$_2$-L^{37}S^{38} or rPAR$_2$-A$^{37\text{-}38}$ were plated in 35 mm dishes and grown for 24 hrs in full 10% serum-containing medium prior to a switch to serum-free medium for a further 16 hours. Cells were then incubated with the PAR$_2$ proteinase agonist trypsin (10nM) or with the synthetic TL sequence-derived peptides like SLIGRL-NH$_2$ (10μM) at 37°C for 10 min. Growth medium was then removed by aspiration and cells were lysed immediately with the addition of cold detergent-containing lysis buffer (complete Lysis-M, Roche, Laval, QC). Lysates were cleared by centrifugation at 4°C for 10 min prior to quantifying protein concentration with a bicinchoninic acid (BCA) protein assay kit (Pierce; Thermo Fisher Scientific, Nepean, ON) using bovine albumin as a standard. Lysates were resolved by electrophoresis in SDS-containing polyacrylamide gels (Biorad, Mississauga, ON) and proteins were transferred to PVDF membranes (GE healthcare, Baie d Urfe, QC) and blocked in detergent-containing tris buffer (TBS-T: 50mM Tris, pH7.4, 150mM NaCl, 0.1% (v/v) Tween 20)

Molecular Pharmacology Fast Forward. Published on July 15, 2009 as DOI: 10.1124/mol.109.055509
This article has not been copyedited and formatted. The final version may differ from this version.

supplemented with 5% non fat milk (TBST/5% milk) for 1 hr at room temperature. ERK/MAPkinase phosphorylation was detected by incubating membranes with phospho-ERK1/2-specific antibodies (New England Biolabs, Pickering, ON) (1/2000 in TBST/5% milk) overnight at 4°C. phospho-ERK immunoreactivity was detected using the secondary horseradish peroxidase (HRP)-conjugated anti mouse antibody (1/15000 in TBST/5% milk for 1hr) and the peroxidase activity was detected by chemiluminescence reagent ECL-plus (GE healthcare, Baie d'Urfe, QC) and film (Kodak). Blots were then stripped by incubation with stripping buffer (Pierce) for 15 min at RT and blocked in TBST/5% milk for 1hr before incubation with total ERK1/2 antibody (New England Biolabs, Pickering, ON) (1/2000 in TBST/5% milk) overnight at 4°C. Total-ERK immunoreactivity was detected using the secondary HRP conjugated anti rabbit antibody (1/15000 in TBST/5% milk for 1 hr) and the peroxidase activity was detected using a chemiluminescence reagent ECL-plus, (GE lifesciences Baie d'Urfe, QC) with X-ray film detection (Kodak) or using a chemiluminescent gel doc system (Biorad, Mississauga, ON). Images were digitized and band intensities were quantified using the imageJ quantification software. Phospho-ERK1/2/phospho-p42/44 MAPkinase levels were normalized for differences in protein loading by expressing the data as a percentage of the corresponding total ERK1/2/p42/44 MAPkinase signal (pERK/tERK; Pp43/44 MAPkinase/Tp43/44 MAPkinase) detected with a pan-MAPkinase/ERK antibody.

In-Cell Western analysis:

For all In-Cell Western analysis, calcium phosphate transfected wild-type or β-arrestin null (DKO) MEF cells were seeded into black, optical bottom 96-well tissue culture treated plates (Nunc, VWR, West Chester, PA), grown to confluence and serum starved overnight, treated with 10 nM Trypsin for 0-90 min at 37°C, and then fixed in normal buffered formalin. Cells were gently permeabilized with phosphate buffered isotonic saline, pH 7.4 (PBS) supplemented with 0.1% Triton X-100, then blocked

Molecular Pharmacology Fast Forward. Published on July 15, 2009 as DOI: 10.1124/mol.109.055509
This article has not been copyedited and formatted. The final version may differ from this version.

for 1 hr with PBS + 1% Fish Gelatin (Sigma). Plates were incubated overnight at 4°C with primary antibody solutions, (pERK: 1:500, Cell signaling; Danvers, MA) and (tERK 1:500, Santa Cruz Biotechnology, Santa Cruz, CA) in PBS containing1% wt/vol. Fish Gelatin. Plates were washed 3 times with PBS, supplemented with 0.5% Tween-20, and then incubated with IR680 and IR800-conjugated secondary antibodies (1:2000) (Li-COR Biosciences, Lincoln, NE) diluted in PBS/1% w/v Fish Gelatin for 1 hr at room temperature. Plates were washed 3 times in PBS-Tween and 1 time in PBS only, and then analyzed using the Odyssey infrared imaging system (LI-COR). Odyssey software was used to calculate integrated intensities of each well for quantification. A fold increase in ERK1/2 phosphorylation (normalized to total ERK levels) over baseline was calculated.

BRET based detection of beta-arrestin interaction with wt-rPAR$_2$ and TL mutated receptors:

The wild-type and mutated receptors (wt-rPAR$_2$, rPAR$_2$-L^{37}S^{38} and rPAR$_2$-A$^{37\text{-}38}$ constructs) were conjugated with YFP at the C-terminus (rPAR$_2$-YFP, rPAR$_2$ L^{37}S^{38}-YFP and rPAR$_2$ A$^{37\text{-}38}$-YFP) and bioluminescence resonance energy transfer (BRET) to renilla luciferase tagged β-arrestin 1 and β-arrestin 2 (Rluc-β-arr1 and Rluc-β-arr2) was determined essentially as previously described (Hamdan et al., 2007). HEK-293 cells were used instead of the KNRK cell line, because the HEK cells provide for a much greater transfection efficiency that is required for the BRET studies. In brief, HEK-293 cells were transiently transfected with 1µg of either rPAR$_2$-YFP, rPAR$_2$ L^{37}S^{38}-YFP or rPAR$_2$ A$^{37\text{-}38}$-YFP along with 0.1µg of the Rluc-β-arr1 or Rluc-β-arr2. Cells were plated in white 96 well culture plates (Perkin Elmer, Waltham, MA) and interactions between the receptors and β-arrestin were detected by BRET following the addition of 5µM coelenterazine (Promega: Madison, WI) on a Mithras fluorescence plate reader (Berthold: Mandel Scientific, Guelph, ON) in luminescence mode using the appropriate filters. The kinetics of β-arrestin recruitment to the receptors was monitored over 20 min.

Microscopy:

Molecular Pharmacology Fast Forward. Published on July 15, 2009 as DOI: 10.1124/mol.109.055509
This article has not been copyedited and formatted. The final version may differ from this version.

HEK cells were plated on glass bottom petri dishes (MatTek Corp. Ashland, MA, USA) and transiently transfected with 1μg of $rPAR_2$-YFP, $rPAR_2$-$L^{37}S^{38}$-YFP or $rPAR_2$-A^{37-38}-YFP constructs. After 48 hrs, the media in the petri dish was replaced with serum-free medium and the cells were treated with Trypsin (10 nM) or SLIGRL-NH_2 (10 μM) for 30 min at 37°C. After fixation of cells with 4% formaldehyde, the cellular localization of the receptor tag YFP signal was detected using an Olympus FV1000 confocal system on an Olympus IX70 microscope with the Fluoview system software. Internalization of cell surface receptor was quantified morphometrically by counting the increased number of intracellular fluorescent speckles per cell in the images, indicative of receptor internalization to endocytic vesicles. To this end, speckles in all cells were counted in a randomly selected representative 40X image, with area dimensions approximately 100 μm x 100 μm (Fig. 9). The average number of speckles per cell was calculated; and the observation was repeated for comparable fields for cells observed in three independently conducted experiments. Data represent the averages of speckles/cell ± s.e.m. for three or more independent experiments.

Statistical Analysis:

Statistical analysis of data and curve fitting were done with Instat and Prism 5 (Graphpad) software. Statistical significance was assessed using the students t test. In the histograms representing the western blot data, averages are shown, ± s.e.m. for three or more independent measurements of band density.

Molecular Pharmacology Fast Forward. Published on July 15, 2009 as DOI: 10.1124/mol.109.055509
This article has not been copyedited and formatted. The final version may differ from this version.

RESULTS

Calcium signaling:

In keeping with our previous work (Kawabata et al., 1999), we observed that activation of wt-rPAR$_2$ by either trypsin or the receptor-selective PAR$_2$-activating peptide, SLIGRL-NH$_2$, stimulates an increase in intracellular calcium in a concentration-dependent manner, with an EC$_{50}$ for trypsin of about 1 nM (Fig 1A) and an EC$_{50}$ for SLIGRL-NH$_2$ of about 5 μM (not shown and see Al-Ani et al., 2004). Reversal of the first two amino acids of the rPAR$_2$ tethered ligand sequence to generate the construct rPAR$_2$-L^{37}S^{38} resulted in a receptor that was unable to recruit calcium signaling following activation by trypsin, but which still remained responsive in terms of calcium signaling upon stimulation by SLIGRL-NH$_2$ (Fig. 1B). Alanine substitution of the first two amino acids in the TL sequence of rPAR$_2$ generated the construct rPAR$_2$ A$^{37-38}$ which like the rPAR$_2$ L^{37}S^{38} construct, failed to trigger an elevation of intracellular calcium when cleaved by trypsin (Fig. 1A), but did yield an intracellular calcium signal in response to SLIGRL-NH$_2$ activation (Fig. 1B). The EC$_{50}$ for SLIGRL-NH$_2$-stimulated calcium signaling by the TL-mutant receptors (EC$_{50}$ ~ 5 μM: data not shown) was equivalent to that for the wild-type receptor, illustrating that the mutations did not affect the ability of the receptor to respond to activating stimuli but rather that the modified trypsin-revealed TL could not promote calcium signaling. Our previous work established that trypsin treatment was able to unmask the mutant TL sequences (Table 1) following the cleavage at the target R^{36}/S^{37} residues (Al-Ani et al., 2004). Alanine substitutions at other positions within the tethered ligand sequence, as previously reported (Al-Ani et al., 2004), resulted in constructs (e.g. rPAR$_2$-A$^{39-42}$, rPAR$_2$-A$^{37-42}$) which show a varying ability to trigger calcium signaling in response to trypsin (data not shown and Al-Ani et al., 2004) and were not investigated further. In keeping with our previous work, all of the synthetic peptides with sequences corresponding to those of the mutated TL receptor sequences (Table 1), (SLAAAA-NH$_2$, AAIGRL-NH$_2$ and LSIGRL-NH$_2$) at

Molecular Pharmacology Fast Forward. Published on July 15, 2009 as DOI: 10.1124/mol.109.055509
This article has not been copyedited and formatted. The final version may differ from this version.

concentrations up to 300 µM failed to trigger a calcium signal (not shown, Supplementary Information and Al-Ani e al., 2004). In view of our results, the focus turned to an evaluation of the two constructs, $rPAR_2$-$L^{37}S^{38}$ and $rPAR_2$-A^{37-38}, which were defective in terms of calcium signaling in response to trypsin, in contrast with the wt-$rPAR_2$ constructs, $rPAR_2$-A^{37-42} and $rPAR_2$-A^{39-42}. Thus, as a TL, the sequences revealed in the clones $rPAR_2$-$L^{37}S^{38}$ and $rPAR_2$-A^{37-38} were unable to activate calcium signaling while $rPAR_2$-A^{37-42} and $rPAR_2$-A^{39-42} could. In contrast none of the corresponding soluble PAR-APs were able to mobilize calcium signaling.

ERK p42/44 MAPkinase signaling:

MAPkinase signaling responses were evaluated in cells expressing the wt-$rPAR_2$ receptor as well as the calcium signaling-defective constructs, $rPAR_2$-$L^{37}S^{38}$ and $rPAR_2$-A^{37-38}. Using increasing concentrations of trypsin, we established that 10nM trypsin consistently stimulated activation of the ERK/p42/44 MAPkinase pathway in the wt-$rPAR_2$ transfected KNRK cells but not in the empty vector transfected KNRK cells (not shown). All other experiments therefore utilized this concentration of trypsin to activate the cells. In order to test the hypothesis that the $rPAR_2$ tethered ligand mutants $rPAR_2$-$L^{37}S^{38}$ and $rPAR_2$-A^{37-38}, while unable to trigger calcium signaling in response to trypsin, might activate MAPkinase, we incubated KNRK cells expressing these constructs with 10nM trypsin. We observed that trypsin stimulated a rapid increase in phospho-p42/44 levels (maximal at 5 to 10 min after trypsin exposure: see Figures 2 and 3) which result was not observed in the empty vector-transfected KNRK cells (Fig. 2). The maximal MAPKinase response seen in cells expressing the TL-mutated PAR_2 constructs was approximately 70% of the response of the wt-$rPAR_2$ transfected cellsl. Since the persistence of the MAPKinase signal is thought to be important for a number of physiological responses, we investigated the time course of MAPKinase activation in cells transfected with wild-type and TL-mutated PAR_2 constructs (Fig. 3). We observed that in all cell lines, 10nM trypsin stimulated a robust

Molecular Pharmacology Fast Forward. Published on July 15, 2009 as DOI: 10.1124/mol.109.055509
This article has not been copyedited and formatted. The final version may differ from this version.

increase in MAPKinase that was maximal after about 5 min, persisted for 40 min and began to decline thereafter, but remained above baseline for at least one hour.

Inhibition of Gq and Gi modestly attenuates MAPkinase activation by trypsin in wt PAR_2 but not in the TL-mutant cell lines:

Since PAR_2-dependent calcium signaling is reported to be Gq-coupled, we evaluated whether the MAPKinase signaling observed in response to activation of the wt-rPAR_2 as well as the tethered ligand mutants rPAR_2-$L^{37}S^{38}$ and rPAR_2-$A^{37\text{-}38}$ by trypsin was dependent on Gq coupling. To suppress Gq signaling, cell lines were treated with the Gαq inhibitor, GP2A (10 μM), (Zoudilova et al., 2007) prior to activation with the same concentration of trypsin that stimulated MAPkinase activation. As a control, the ability of GP2A to block trypsin-triggered calcium signaling in the wt-rPAR_2 KNRK cell line was tested. Since neither of the mutated TL PAR_2 cell lines signal via calcium when activated by trypsin, they were not tested in this way. Efficient (>90%) inhibition of Gq-mediated calcium signaling was observed in terms of the complete suppression of trypsin-triggered effects by 10 μM GP2A in the wt-rPAR_2 cell line (not shown). However, in the wt-PAR_2 cell line, the Gq inhibitor caused only a modest inhibition (about 30%) of trypsin-triggered MAPkinase activation (Fig. 4b). In contrast, under the same conditions in the presence of the Gq inhibitor, GP2A, we observed no difference in the ability of trypsin to activate the p42/44 MAPKinase pathway in the two cell lines with mutated TL sequence (rPAR_2 $L^{37}S^{38}$ and rPAR_2 $A^{37\text{-}38}$: Fig. 5 and Fig. 6). This lack of inhibition of MAPKinase activation was in contrast with the ability of GP2A to block SLIGRL-NH_2-mediated calcium signaling in the rPAR_2 $L^{37}S^{38}$ and rPAR_2 $A^{37\text{-}38}$-expressing cells (not shown). Thus, although upon PAR-AP activation, the mutant receptors can engage Gq to promote calcium mobilization, the activation of Gq was not involved in the ability of these receptors to activate ERK1/2 when stimulated by trypsin. Further, treatment of cells with pertussis toxin (PTX: 100 ng/ml; 16 hrs) to compromise Gi coupling had no effect on the

Molecular Pharmacology Fast Forward. Published on July 15, 2009 as DOI: 10.1124/mol.109.055509
This article has not been copyedited and formatted. The final version may differ from this version.

ability of trypsin or SLIGRL-NH_2 to cause calcium signaling in all three cell lines (not shown). In the TL-mutant cell lines, PTX treatment was similarly ineffective in blocking trypsin-activated MAPkinase signaling, although in the wt-PAR_2 cell line, PTX caused a small (about 30%) inhibition of trypsin-triggered MAPkinase activation (Figs. 4 to 6). Thus, we concluded that in the TL-mutant cell lines, trypsin-mediated MAPkinase activation was independent of both Gi and Gq coupling, whereas in the wt-PAR_2 cell line, MAPkinase activation by trypsin was partially Gq and Gi-dependent.

PAR_2 mediated activation of MAPkinase does not involve trans-activation of the EGF receptor (EGFR):

In view of the ability of PAR_2, like other G-protein-coupled receptors, to cause signaling by trans-activation of the EGF receptor (EGFR) (Darmoul et al., 2004; Daub et al., 1996; McCole et al., 2002; van der Merwe et al., 2008) we tested the hypothesis that EGFR transactivation triggered by the metalloproteinase-catalysed release of an EGFR ligand (HB-EGF or TGF-α) might be involved in trypsin-mediated activation of either calcium signaling or MAPkinase in the wild-type or mutant TL-PAR_2 cell lines. In KNRK cells transfected with wt-rPAR_2, neither the EGFR kinase inhibitor, AG1478 (1μM), nor the broad spectrum matrix metalloproteinase (MMP) inhibitor, doxycycline (0.1 mM) inhibited calcium signaling activated by trypsin (not shown). Further, neither AG1478 nor doxycycline had any effect on MAPkinase activation in any of the cell lines tested (Figs. 4 to 6). These results argued strongly against a role for trans-activation of the EGFR in the activation of MAPkinase by trypsin in the PAR_2-expressing KNRK cell lines.

Involvement of Src and Rho-Kinase in trypsin-mediated activation of MAPKinase:

To asses the potential role of Src and Rho kinase in mediating PAR_2 signaling, we tested the ability of the Src-selective inhibitor, PP1 (Hanke et al., 1996) and the Rho kinase inhibitor Y27362 **(**10 μM)

Molecular Pharmacology Fast Forward. Published on July 15, 2009 as DOI: 10.1124/mol.109.055509
This article has not been copyedited and formatted. The final version may differ from this version.

(Uehata et al., 1997), to attenuate trypsin-mediated MAPkinase activation. As shown in Figs. 4 to 6, the Src-kinase inhibitor inhibited MAPkinase activation by about 30% in the wt-rPAR$_2$ cell line (Fig. 4), but had no effect on trypsin-mediated MAPkinase activation in the TL mutant cell lines (Figs. 5 and 6). In contrast, the Rho kinase inhibitor blocked trypsin-triggered activation by over 80% in all cell lines. Similar results were observed with the more potent Rho-kinase inhibitor H1152 (1 μM, not shown). In order to determine whether the Rho kinase dependent signal observed was downstream of G12/13, we over expressed constructs encoding Gα12 and Gα13 into KNRK cells stably expressing rPAR$_2$-L$^{37\text{-}38}$. We note an increased sensitivity to trypsin activation of MAPK in these cells with a signal observed with exposure to 5nM trypsin, which is absent in control cells not over expressing Gα12 and Gα13 (Fig. 7). Similar results were observed with the rPAR$_2$-A$^{37\text{-}38}$ (not shown).

Beta-arrestin interactions and PAR$_2$-mediated MAPkinase signaling:

Previous work has pointed to a role for beta arrestin in facilitating a prolonged activation of MAPkinase by PAR$_2$ (Ge et al., 2003), and it has been proposed that PAR$_2$ may trigger responses distinct from a Gq coupled elevation of intracellular calcium by a β-arrestin-mediated pathway (Zoudilova et al., 2007). We therefore tested the potential role(s) of β-arrestins in trypsin-mediated MAPkinase activation in the different PAR$_2$ cell lines. To evaluate the role(s) of β-arrestins we assessed MAPkinase signaling triggered by trypsin in β-arrestin-null murine embryo fibroblasts (double-knockout murine embryo fibroblasts: DKO MEF) transfected with the wt-rPAR$_2$-YFP and the TL mutated constructs, rPAR$_2$-L^{37}S^{38}-YFP and rPAR$_2$-A$^{37\text{-}38}$-YFP. When expressed in the DKO MEF background, all receptor constructs showed an increase in MAPkinase activation in response to trypsin as was observed in the KNRK cells. MAPKinase activation was greater for wt-rPAR$_2$ (about 6-fold over baseline) than for both of the TL-mutated constructs (2-4 fold over baseline) (Fig. 8, upper panel A-C). However, in the β-arrestin DKO MEF cells expressing wt-rPAR$_2$, a reduction in the magnitude of the trypsin-activated

Molecular Pharmacology Fast Forward. Published on July 15, 2009 as DOI: 10.1124/mol.109.055509
This article has not been copyedited and formatted. The final version may differ from this version.

MAPkinase signal was observed (~2 fold over baseline), while MAPKinase activation by the TL-mutated receptors was similar to that observed in wt-MEF's (~2 fold for rPAR$_2$-A$^{37-38}$-YFP and ~3 fold for rPAR$_2$-L^{37}S^{38}-YFP). (Fig. 8, panels B-C). Thus, the MAPkinase activation by wt-rPAR$_2$ appeared to be partially β-arrestin-dependent, whereas the magnitude of MAPkinase activation caused by trypsin activation of the PAR$_2$-A$^{37-38}$ and PAR$_2$-L^{37}S^{38} receptors appeared to be principally independent of the expression of the two β-arrestins.

Trypsin-activated wt-rPAR$_2$-YFP interacts with beta-arrestins whereas trypsin-activated rPAR$_2$-L^{37}S^{38}-YFP and rPAR$_2$-A$^{37-38}$-YFP do not:

The above result suggested that in contrast to the wt-rPAR$_2$, the trypsin-activated mutant forms of the receptor might not recruit β-arrestin. To test this possibility we used a bioluminescence resonance energy transfer method (BRET) approach to monitor the interactions of β-arrestin-1 and β-arrestin-2 with wt-rPAR$_2$, rPAR$_2$-L^{37}S^{38}-YFP or rPAR$_2$-A$^{37-38}$-YFP upon activation of the receptors either by trypsin or by the PAR$_2$-activating peptide, SLIGRL-NH$_2$. We observed that when stimulated with trypsin (Fig. 9 and Supplementary Information), only the wild-type rPAR$_2$ showed a time-dependent increase in BRET, indicating interactions with both β-arrestin 1 (not shown and Supplementary Information) and β-arrestin 2 (Fig. 9A). The BRET signals for the interaction of wild-type rPAR$_2$ with both β-arrestins 1 and 2 were comparable, whether activated by trypsin or the PAR-activating peptide, SLIGRL-NH$_2$ (Fig. 9B versus 9A and data not shown for β-arrestin 1: see Supplementary Information). In contrast, activation of rPAR$_2$-L^{37}S^{38}-YFP or rPAR$_2$-A$^{37-38}$-YFP with trypsin failed to generate a BRET signal with either of β-arrestins 1 or 2 (Figures 9C, 9D and data not shown for β-arrestins 1: see Supplementary Information). Notwithstanding, activation of the TL-mutant receptors with the PAR$_2$-activating peptide, SLIGRL-NH$_2$, was able to generate a BRET signal for the recruitment of either β-arrestin 1 (not shown and see Supplementary Information) or β-arrestin 2 (inserts, Figs. 9C and 9D),

Molecular Pharmacology Fast Forward. Published on July 15, 2009 as DOI: 10.1124/mol.109.055509
This article has not been copyedited and formatted. The final version may differ from this version.

respectively. Thus, although the two TL-mutant receptors were in principle able to interact with both β-arrestins 1 and 2 (activation by SLIGRL-NH_2), the trypsin-exposed mutant TL sequences failed to promote a receptor- β-arrestin interaction, as reflected by the BRET measurements.

Impaired internalization of TL-mutated PAR_2 receptors following trypsin activation:

β-arrestin interaction is known to be critical for internalization of PAR_2 (Ge et al., 2003). Since we observed impaired β-arrestin interaction with the TL-modified PAR_2 constructs, we wished to investigate the internalization of wt-rPAR_2, rPAR_2-$L^{37}S^{38}$ and rPAR_2-$A^{37\text{-}38}$ following activation with trypsin and SLIGRL-NH_2. To evaluate agonist-triggered receptor internalization, we elected to use an HEK cell background, because of the much higher efficiency of receptor transfection in these cells, compared with the KNRK cells. wt-rPAR_2-YFP, rPAR_2-$L^{37}S^{38}$-YFP or rPAR_2-$A^{37\text{-}38}$-YFP transiently transfected in HEK cells were treated with agonists for 30 min and receptor internalization was quantified by morphometric analysis as described in Materials and Methods. We observed that the wt-rPAR_2 receptor showed significant internalization following both trypsin (10nM) and SLIGRL-NH_2 (10μM) activation, with the magnitude of trypsin-triggered internalization approaching that of internalization triggered by the synthetic activating peptide (10A: ii, iii and Fig. 10B). In contrast, trypsin-mediated internalization of the TL-mutant receptors was markedly diminished, relative to that of the wild-type receptor (Fig 10A, v, vi; viii, ix; 10B), whereas SLIGRL-NH_2-activated internalization of the rPAR_2-$L^{37}S^{38}$-YFP and rPAR_2-$A^{37\text{-}38}$-YFP receptors was equivalent to peptide-triggered internalization of the wild-type receptor.

Molecular Pharmacology Fast Forward. Published on July 15, 2009 as DOI: 10.1124/mol.109.055509
This article has not been copyedited and formatted. The final version may differ from this version.

SLAAAA-NH_2 as a biased agonist for PAR_2:

We observed that the trypsin-revealed N-terminal sequence of the PAR_2 mutant, PAR_2-A^{39-42} (exposed TL sequence: SLAAAA---) could signal to both calcium (Al-Ani et al., 2004 and data not shown) and MAPKinase (not shown and Supplementary Information), but that the corresponding TL-derived synthetic soluble peptide, SLAAAA-NH_2 could not cause PAR_2-mediated calcium signaling (Al-Ani et al., 2004 and data not shown). We thus wondered if this peptide might be able to cause biased signaling by PAR_2 so as to activate MAPKinase. Although it could not cause an elevation of intracellular calcium, this peptide was able to stimulate MAPkinase activation in both the wild-type and mutated receptor constructs (Figure 11). In contrast, the peptides AAIGRL-NH_2 and LSIGRL-NH_2, corresponding to the revealed TL sequences in PAR_2-A^{37-38} and PAR_2-$L^{37}S^{38}$, were not able to activate either calcium (not shown) or MAPkinase signaling (Figure 10, top panel).

DISCUSSION

The main finding of our study was that distinct trypsin-revealed PAR_2 tethered ligand sequences can act as biased agonists to activate different signaling pathways selectively. Further, we found that selective activation of MAPKinase versus calcium signaling, can occur either via a proteolytically-revealed tethered ligand with a mutated receptor-activating sequence or via a synthetic soluble PAR_2 peptide agonist. Given the unusual proteolytic mechanism of activation of PAR_2, these results represent a unique tethered ligand mechanism of 'biased agonism' that has been documented for a variety of other G-protein-coupled receptors that are activated by soluble ligands (Galandrin et al., 2007; Kenakin, 2007; Urban et al., 2007; Wei et al., 2003).

Structure-activity profile for the trypsin-revealed tethered ligand sequence and MAPkinase activation.

In our earlier work studying the roles of the tethered ligand and extracellular loop 2 for PAR_2 signaling,

Molecular Pharmacology Fast Forward. Published on July 15, 2009 as DOI: 10.1124/mol.109.055509
This article has not been copyedited and formatted. The final version may differ from this version.

we only used calcium signaling as an index of receptor activation (Al-Ani et al., 1999; Al-Ani et al., 2002). That work pointed to differences between the interactions of the extracellular receptor domains with the proteolytically revealed tethered ligand, compared with the comparable soluble synthetic PAR-activating peptides. We were able to conclude that several distinct sites on the extracellular domains of PAR_2 can interact with TL amino acid sequences either as the intact TL or as synthetic peptides to trigger calcium signaling. We showed further, that the first two amino acids of the revealed TL of PAR_2 (SL----) play a major role in triggering calcium signaling (Al-Ani et al., 2004), but the impact of those two revealed amino acids on MAPkinase activation was not assessed. Our current work shows that when the SL sequence in the revealed TL is replaced by alanines ($rPAR_2$-A^{37-38}) or if the residues are simply switched in sequence ($rPAR_2$-$L^{37}S^{38}$), the ability of the revealed tethered ligand to stimulate an elevation of intracellular calcium is lost, but the activation of MAPkinase is retained. This agonist-biased signaling by the trypsin-revealed TL, with a triggering of MAPkinase but not calcium, was also observed for the synthetic PAR-activating peptide, SLAAAA-NH_2, but not for AAIGRL-NH_2 or LSIGRL-NH_2 that were inactive for both pathways. Thus, SLAAAA-NH_2 is a biased agonist for PAR_2 and its ability to interact with the receptor appears to differ from that of the same sequence when presented to the receptor as a trypsin-revealed tethered ligand, which can activate both calcium and MAPkinase signaling.

MAPkinase activation and interaction with arrestins. Based on previous observations indicating a role for β-arrestin in regulating PAR_2 stimulated MAPKinase signaling (Defea, 2008; Ge et al., 2003; Zoudilova et al., 2007), we hypothesized that all receptor variants that can activate MAPkinase in the absence of Ca^{2+} mobilization would do so via interaction with β-arrestins. It was thus surprising that the receptor mutants did not interact with β-arrestins 1 and 2 when triggered by trypsin (Figs. 8C, 8D and Supplementary Information). Furthermore, while the magnitude of MAPKinase activation by the wt-

Molecular Pharmacology Fast Forward. Published on July 15, 2009 as DOI: 10.1124/mol.109.055509
This article has not been copyedited and formatted. The final version may differ from this version.

rPAR$_2$ was greater than for the TL-mutated receptors when transfected into wt-MEFs, all three receptors promoted similar levels of MAPKinase activation in the absence of β-arrestins (Figs. 8B, 8C). These data suggest that trypsin-activated wt-rPAR$_2$ can activate MAPkinase by both a β-arrestin-dependent and β-arrestin-independent mechanism, whereas the mutated receptors, upon trypsin activation, can trigger MAPkinase principally via a β-arrestin-independent mechanism. Notwithstanding, activation of all receptor variants by the soluble PAR-activating peptide appears to trigger MAPkinase by both the arrestin-dependent and -independent pathways, suggesting that the tethered ligand mutations do not affect the overall signaling ability of these mutants, but rather the binding of the mutant tethered ligand domain promotes a distinct set of responses. This dual process for MAPkinase activation by PAR$_2$ mirrors the ability of various beta-adrenergic receptor-targeted ligands to activate MAPkinase by distinct mechanisms (Galandrin et al., 2008).

As previously reported wt-PAR$_2$ interacts with β-arrestins 1 and 2 and our BRET based analysis of this interaction revealed that PAR$_2$ is a class B GPCR that interacts stably with and is co-internalized with β-arrestin (Hamdan et al., 2005). This stable interaction is likely due to the presence of Serine and Threonine clusters in the C-tail of PAR$_2$ (residues 380-397), as has been reported for a number of other GPCRs (Oakley et al., 2001).

Trypsin versus PAR-activating peptide-stimulated receptor internalization and the ability of receptors to interact with arrestins. Since the interaction of PAR$_2$ with β-arrestin is critical for PAR$_2$ internalization (DeFea et al., 2000) and since the internalized receptor scaffold plays an important role in PAR$_2$-mediated signaling and chemotaxis (Ge et al., 2003; Zoudilova et al., 2007), we anticipated differences in internalization between the trypsin-activated receptor constructs that did and did not interact with beta arrestins (presence or absence of BRET signals in Fig. 9). Indeed, whereas trypsin triggered internalization of the wild-type PAR$_2$ to an extent comparable to that triggered by the PAR$_2$-

Molecular Pharmacology Fast Forward. Published on July 15, 2009 as DOI: 10.1124/mol.109.055509
This article has not been copyedited and formatted. The final version may differ from this version.

activating peptide (Fig. 10, panels ii and iii), there was only minimal trypsin-triggered internalization of the mutated receptors, PAR_2-$L^{37}S^{38}$ and PAR_2-A^{37-38} (Fig. 10, panels v and viii). In contrast, morphometric analysis of receptor internalization (Fig. 10B) demonstrated that the PAR_2-activating peptide caused an equivalent internalization of all receptor constructs (Fig. 10A, panels iii, vi and ix and Fig. 9B). These observations correlated very well with the ability of SLIGRL-NH_2, but not trypsin, to stimulate interactions between the TL-mutated receptors and β-arrestins (Fig. 9).

Signaling pathways and activation of MAPkinase by trypsin-stimulated receptors. Given the β-arrestin independence of trypsin-mediated activation of MAPkinase by the mutated receptors, our focus turned to other signal pathways. Unlike other GPCR-triggered MAPkinase activation, the PAR_2-stimulated process was not affected by either doxycycline or the EGF receptor kinase inhibitor AG1478/ PD153035 (Figs. 4 to 6). Those data indicated that the predominant PAR_2 mechanism for activating MAPkinase in the KNRK cell background does not involve either the metalloproteinase (MMP)-mediated release of an EGF receptor agonist (Daub et al., 1996) or an MMP-independent trans-activation of the EGF receptor. The inhibition of either Gq (GP2A) or Gi (PTX treatment) had no effect on MAPkinase stimulation by the trypsin-activated mutated receptors, PAR_2-A^{37-38} or PAR_2-$L^{37}S^{38}$ and had only a very modest effect (about 30% inhibition) on trypsin-mediated activation of MAPkinase by the wt-rPAR_2. Similarly, the Src-targeted inhibitor, PP1, had no effect on trypsin-triggered activation of MAPkinase by the two mutated receptors and only a small inhibitory effect (about 30%) on MAPkinase activation by the wild-type receptor (Figs. 4 to 6). Thus, in the KNRK cell background, the process of proteinase-mediated PAR_2-stimulated MAPkinase activation appeared to be largely independent of pathways involving many of the common signal components (Gq, Gi, Src, EGFR). That said, the Rho kinase inhibitors, Y27362 and H1152 had a major inhibitory effect on the ability of all PAR_2 constructs to stimulate MAPkinase when activated by trypsin (Figs. 4-6). The role of Rho kinase in activation of

Molecular Pharmacology Fast Forward. Published on July 15, 2009 as DOI: 10.1124/mol.109.055509
This article has not been copyedited and formatted. The final version may differ from this version.

MAPkinase by PAR_2 is in keeping with the role of this kinase for the activation of MAPkinase and other responses by PAR_1 (Carbajal et al., 2000; McLaughlin et al., 2005; Seasholtz et al., 1999; Vouret-Craviari et al., 1998) and PAR_2 (Scott et al., 2003). Over expression of constructs encoding Gα12 and Gα13 resulted in an increase in trypsin sensitivity of the cells to MAPK signaling suggesting that the Rho kinase dependent MAPK signal seen in these cells is G12/13 dependent (Fig. 7). Thus, in future work with intact tissue PAR_2 targets (e.g. vasculature, neurons) it will be of considerable importance to evaluate the potential role of Rho kinase and G12/13 dependent signaling events.

We found that like the distinct trypsin-revealed tethered ligands, synthetic soluble PAR-activating peptides are also capable of agonist-biased signaling by PAR_2. Specifically, SLIGRL-NH_2 was able to trigger both an elevation of intracellular calcium and an activation of MAPkinase, whereas SLAAAA-NH_2 triggers only MAPkinase activation (Fig. 11), without causing a calcium signal (Al-Ani et al., 2004). In contrast with the trypsin-revealed mutated tethered ligands with the sequences, AAIGRL--- (PAR_2-A^{37-38}) and LSIGRL--- (PAR_2-$L^{37}S^{38}$), the analogous synthetic peptides with the sequences, AAIGRL-NH_2 and LSIGRL-NH_2 were unable to activate either MAPkinase or calcium signaling. These results indicate that the tethered and soluble ligands most likely bind differentially and/or stabilize different conformations of the receptor leading to the activation of distinct subsets of signaling cascades. Further work will be needed to understand better the specific structural basis of this biased signaling.

In summary, we describe agonist-biased signaling by both a trypsin-revealed tethered ligand and a synthetic PAR_2-activating peptide that can lead to the selective activation of MAPkinase versus calcium signaling by PAR_2 as well as distinctions in recruitment of β-arrestin and receptor endocytosis. The ability of the PAR-activating peptide, SLAAAA-NH_2 to signal selectively via MAPkinase versus calcium establishes in principle the possibility of developing signal-selective PAR_2 agonists that may be of therapeutic utility.

Molecular Pharmacology Fast Forward. Published on July 15, 2009 as DOI: 10.1124/mol.109.055509
This article has not been copyedited and formatted. The final version may differ from this version.

References

Al-Ani B, Hansen KK and Hollenberg MD (2004) Proteinase-activated receptor-2: key role of amino-terminal dipeptide residues of the tethered ligand for receptor activation. *Mol Pharmacol* **65**(1):149-156.

Al-Ani B, Saifeddine M, Kawabata A and Hollenberg MD (1999) Proteinase activated receptor 2: Role of extracellular loop 2 for ligand-mediated activation. *Br J Pharmacol* **128**(5):1105-1113.

Al-Ani B, Wijesuriya SJ and Hollenberg MD (2002) Proteinase-activated receptor 2: differential activation of the receptor by tethered ligand and soluble peptide analogs. *J Pharmacol Exp Ther* **302**(3):1046-1054.

Bohm SK, Kong W, Bromme D, Smeekens SP, Anderson DC, Connolly A, Kahn M, Nelken NA, Coughlin SR, Payan DG and Bunnett NW (1996) Molecular cloning, expression and potential functions of the human proteinase-activated receptor-2. *Biochem J* **314 (Pt 3)**:1009-1016.

Carbajal JM, Gratrix ML, Yu CH and Schaeffer RC, Jr. (2000) ROCK mediates thrombin's endothelial barrier dysfunction. *Am J Physiol Cell Physiol* **279**(1):C195-204.

Chen C and Okayama H (1987) High-efficiency transformation of mammalian cells by plasmid DNA. *Mol Cell Biol* **7**(8):2745-2752.

Darmoul D, Gratio V, Devaud H and Laburthe M (2004) Protease-activated receptor 2 in colon cancer: trypsin-induced MAPK phosphorylation and cell proliferation are mediated by epidermal growth factor receptor transactivation. *J Biol Chem* **279**(20):20927-20934.

Daub H, Weiss FU, Wallasch C and Ullrich A (1996) Role of transactivation of the EGF receptor in signalling by G-protein-coupled receptors. *Nature* **379**(6565):557-560.

Defea K (2008) Beta-arrestins and heterotrimeric G-proteins: collaborators and competitors in signal transduction. *Br J Pharmacol* **153 Suppl 1**:S298-309.

DeFea KA, Zalevsky J, Thoma MS, Dery O, Mullins RD and Bunnett NW (2000) beta-arrestin-dependent endocytosis of proteinase-activated receptor 2 is required for intracellular targeting of activated ERK1/2. *J Cell Biol* **148**(6):1267-1281.

Dulon S, Cande C, Bunnett NW, Hollenberg MD, Chignard M and Pidard D (2003) Proteinase-activated receptor-2 and human lung epithelial cells: disarming by neutrophil serine proteinases. *Am J Respir Cell Mol Biol* **28**(3):339-346.

Dulon S, Leduc D, Cottrell GS, D'Alayer J, Hansen KK, Bunnett NW, Hollenberg MD, Pidard D and Chignard M (2005) Pseudomonas aeruginosa elastase disables proteinase-activated receptor 2 in respiratory epithelial cells. *Am J Respir Cell Mol Biol* **32**(5):411-419.

Galandrin S, Oligny-Longpre G, Bonin H, Ogawa K, Gales C and Bouvier M (2008) Conformational rearrangements and signaling cascades involved in ligand-biased mitogen-activated protein kinase signaling through the beta1-adrenergic receptor. *Mol Pharmacol* **74**(1):162-172.

Galandrin S, Oligny-Longpre G and Bouvier M (2007) The evasive nature of drug efficacy: implications for drug discovery. *Trends Pharmacol Sci* **28**(8):423-430.

Ge L, Ly Y, Hollenberg M and DeFea K (2003) A beta-arrestin-dependent scaffold is associated with prolonged MAPK activation in pseudopodia during protease-activated receptor-2-induced chemotaxis. *J Biol Chem* **278**(36):34418-34426.

Hamdan FF, Audet M, Garneau P, Pelletier J and Bouvier M (2005) High-throughput screening of G protein-coupled receptor antagonists using a bioluminescence resonance energy transfer 1-based beta-arrestin2 recruitment assay. *J Biomol Screen* **10**(5):463-475.

Hamdan FF, Rochdi MD, Breton B, Fessart D, Michaud DE, Charest PG, Laporte SA and Bouvier M (2007) Unraveling G protein-coupled receptor endocytosis pathways using real-time monitoring

of agonist-promoted interaction between beta-arrestins and AP-2. *J Biol Chem* **282**(40):29089-29100.

Hanke JH, Gardner JP, Dow RL, Changelian PS, Brissette WH, Weringer EJ, Pollok BA and Connelly PA (1996) Discovery of a novel, potent, and Src family-selective tyrosine kinase inhibitor. Study of Lck- and FynT-dependent T cell activation. *J Biol Chem* **271**(2):695-701.

Kawabata A, Saifeddine M, Al-Ani B, Leblond L and Hollenberg MD (1999) Evaluation of proteinase-activated receptor-1 (PAR1) agonists and antagonists using a cultured cell receptor desensitization assay: activation of PAR2 by PAR1-targeted ligands. *J Pharmacol Exp Ther* **288**(1):358-370.

Kenakin T (2007) Collateral efficacy in drug discovery: taking advantage of the good (allosteric) nature of 7TM receptors. *Trends Pharmacol Sci* **28**(8):407-415.

McCole DF, Keely SJ, Coffey RJ and Barrett KE (2002) Transactivation of the epidermal growth factor receptor in colonic epithelial cells by carbachol requires extracellular release of transforming growth factor-alpha. *J Biol Chem* **277**(45):42603-42612.

McLaughlin JN, Shen L, Holinstat M, Brooks JD, Dibenedetto E and Hamm HE (2005) Functional selectivity of G protein signaling by agonist peptides and thrombin for the protease-activated receptor-1. *J Biol Chem.*

Nystedt S, Emilsson K, Wahlestedt C and Sundelin J (1994) Molecular cloning of a potential proteinase activated receptor. *Proc Natl Acad Sci U S A* **91**(20):9208-9212.

Oakley RH, Laporte SA, Holt JA, Barak LS and Caron MG (2001) Molecular determinants underlying the formation of stable intracellular G protein-coupled receptor-beta-arrestin complexes after receptor endocytosis. *J Biol Chem* **276**(22):19452-19460.

Scott G, Leopardi S, Parker L, Babiarz L, Seiberg M and Han R (2003) The proteinase-activated receptor-2 mediates phagocytosis in a Rho-dependent manner in human keratinocytes. *J Invest Dermatol* **121**(3):529-541.

Seasholtz TM, Majumdar M, Kaplan DD and Brown JH (1999) Rho and Rho kinase mediate thrombin-stimulated vascular smooth muscle cell DNA synthesis and migration. *Circ Res* **84**(10):1186-1193.

Uehata M, Ishizaki T, Satoh H, Ono T, Kawahara T, Morishita T, Tamakawa H, Yamagami K, Inui J, Maekawa M and Narumiya S (1997) Calcium sensitization of smooth muscle mediated by a Rho-associated protein kinase in hypertension. *Nature* **389**(6654):990-994.

Urban JD, Clarke WP, von Zastrow M, Nichols DE, Kobilka B, Weinstein H, Javitch JA, Roth BL, Christopoulos A, Sexton PM, Miller KJ, Spedding M and Mailman RB (2007) Functional selectivity and classical concepts of quantitative pharmacology. *J Pharmacol Exp Ther* **320**(1):1-13.

van der Merwe JQ, Hollenberg MD and MacNaughton WK (2008) EGF receptor transactivation and MAP kinase mediate proteinase-activated receptor-2-induced chloride secretion in intestinal epithelial cells. *Am J Physiol Gastrointest Liver Physiol* **294**(2):G441-451.

Vouret-Craviari V, Boquet P, Pouyssegur J and Van Obberghen-Schilling E (1998) Regulation of the actin cytoskeleton by thrombin in human endothelial cells: role of Rho proteins in endothelial barrier function. *Mol Biol Cell* **9**(9):2639-2653.

Wei H, Ahn S, Shenoy SK, Karnik SS, Hunyady L, Luttrell LM and Lefkowitz RJ (2003) Independent beta-arrestin 2 and G protein-mediated pathways for angiotensin II activation of extracellular signal-regulated kinases 1 and 2. *Proc Natl Acad Sci U S A* **100**(19):10782-10787.

Zoudilova M, Kumar P, Ge L, Wang P, Bokoch GM and Defea KA (2007) beta-Arrestin-dependent Regulation of the Cofilin Pathway Downstream of Protease-activated Receptor-2. *J Biol Chem* **282**(28):20634-20646.

Footnotes:

These studies were supported in part by operating grants from the Canadian Institutes of Health Research and the US National Institutes of Health and by a Canadian Association of Gastroenterology/Canadian Institutes of Health Research/Ortho-Jensen post-doctoral fellowship.

Molecular Pharmacology Fast Forward. Published on July 15, 2009 as DOI: 10.1124/mol.109.055509
This article has not been copyedited and formatted. The final version may differ from this version.

Figure Legends

Figure 1: Trypsin does not activate calcium signaling in the TL-mutant PAR_2 receptors as it does in wt-$rPAR_2$: comparison with activation by SLIGRL-NH_2. (A) Concentration-effect curves for trypsin-triggered calcium signaling. Receptor-expressing KNRK cell lines (■, wt-PAR_2; ●, $rPAR_2$-A^{37-38}; ◆, $rPAR_2$-$L^{37}S^{38}$; □, pcDNA3) were exposed to trypsin at increasing concentrations and the elevation of intracellular calcium relative to the signal caused by 1 μM A23187 (% A23187) was monitored as described in Materials and Methods. (A) Trypsin concentration-effect curve for calcium signaling and (B) Calcium signaling (% A23187) triggered by SLIGRL-NH_2 (300 μM) in wt-$rPAR_2$ (■), $rPAR_2$-$L^{37}S^{38}$ (◆) and $rPAR_2$-A^{37-38} (●) transfected KNRK cells. Values at each trypsin concentration (A) and in the histograms (B) represent the averages (± s.e.m., Bars) for three or more independently conducted experiments.

Figure 2: Trypsin-mediated activation of MAPkinase in KNRK cell lines expressing wild-type and TL-mutant PAR_2. (A) *Upper:* Representative western blots showing activation of p42/44 MAPkinase in wt-$rPAR_2$, $rPAR_2$-$L^{37}S^{38}$, $rPAR_2$-A^{37-38} and pcDNA3 transfected KNRK cell lines in response to stimulation by 10nM trypsin for 10 min. **(B)** *Lower:* Quantitative densitometric image analysis of p42/44 MAPkinase activation (Phospho p42/44 western blot signal), relative to total p42/44 MAPkinase (total-p42/44 signal, upper panel) in wt-$rPAR_2$, $rPAR_2$-$L^{37}S^{38}$, $rPAR_2$-A^{37-38} and pcDNA3 transfected KNRK cells in response to stimulation by trypsin (10 nM) for 10 min. * denotes a significant ($P< 0.01$) increase in Phospho p42/44 compared with baseline values. Data are representative of three independent experiments.

Figure 3: Time course of trypsin-triggered MAPkinase activation by wild-type and TL-mutant PAR_2. (A**)** Representative western blots showing the time course (minutes) for p42/44 MAPkinase

Molecular Pharmacology Fast Forward. Published on July 15, 2009 as DOI: 10.1124/mol.109.055509
This article has not been copyedited and formatted. The final version may differ from this version.

activation (P-p42/44) by trypsin in wt-rPAR$_2$ and TL modified rPAR$_2$ transfected KNRK cell lines, compared with total MAPkinase (T-p42/44). **(B)** Quantitative densitometric image analysis for the percentage increase of MAPKinase activation phospho(P)-p42/44 over baseline, normalized to total(T)-p42/44 levels following activation by trypsin in wt rPAR$_2$ and TL-modified rPAR$_2$ transfected KNRK cell lines. Data represent the average values (± s.e.m., Bars) for three or more independently conducted experiments.

Figure 4: Effects of inhibitors on trypsin stimulated MAPkinase signaling in wt-rPAR$_2$ KNRK cells. KNRK cells expressing wt-rPAR$_2$ were activated by trypsin (10 nM, 10 min.) in the absence or presence of the indicated inhibitors, followed by western blot analysis of MAPkinase activation (Phospho(P)-p42/44), relative to total enzyme (T-p42/44). **(A)** Representative western blots visualizing activated (top gel: phospho(P)-p42/4) and total enzyme (lower gel: total(T)-p42/44). **(B)** Quantitative densitometric image analysis for the percentage increase over baseline of phospho(P)-p42/44 normalized to total(T)-p42/44, integrating the signal for both bands visualized for Phospho(P)-p42/44, relative to total(T)-p42/44. The superscripts, *, ** and *** denote a significant increase (*, $P<0.05$; **$P<0.01$, ***$P<0.001$) compared with unstimulated cells (NT). # and ## denotes a significant decrease (#, $P<0.15$; ## $P<0.01$) between the stimulation by trypsin in the presence of the Rho-Kinase inhibitor, Y27362, compared with cells stimulated by trypsin in the absence of the inhibitor. Data are representative of three independent experiments

Figure 5: Selective impact of a Rho kinase inhibitor compared with other inhibitors on trypsin stimulated MAPkinase signaling in rPAR$_2$-L^{37}S^{38} KNRK cells. Experiments identical to the ones outlined in Figure 4 were done using rPAR$_2$-L^{37}S^{38} KNRK cells. **(A)** Representative western blots visualizing activated MAPkinase (top gel: phospho(P)-p42/4) and total enzyme (lower gel: total(T)-p42/44). **(B)** Quantitative densitometric image analysis of MAPkinase activation expressed as the

Molecular Pharmacology Fast Forward. Published on July 15, 2009 as DOI: 10.1124/mol.109.055509
This article has not been copyedited and formatted. The final version may differ from this version.

percentage increase over baseline (no treatment: NT) of phospho(P)-p42/44 normalized to total(T)p42/44. The superscripts, *, ** and *** denote a significant increase (*, P<0.05; **P<0.01, ***P<0.001) compared with unstimulated cells (NT). ## denotes a significant decrease (P<0.01) for the stimulation by trypsin (10 nM) in the presence of the Rho-Kinase inhibitor, Y27362 (10 μM), compared with cells stimulated by trypsin in the absence of the inhibitor. Data are representative of three independent experiments.

Figure 6: Selective impact of a Rho kinase inhibitor compared with other inhibitors on trypsin stimulated MAPkinase signaling in rPAR$_2$-A$^{37\text{-}38}$ KNRK cells. Experiments identical to the ones outlined in Figure 4 were done using rPAR$_2$-L^{37}S^{38} KNRK cells. **(A)** Representative western blots visualizing activated (top gel: phospho(P)-p42/44) and total enzyme (lower gel: total(T)-p42/44). **(B)** Quantitative densitometric image analysis of MAPkinase activation expressed as the percentage increase over baseline (no treatment: NT) of phospho(P)-p42/44 normalized to total(T)p42/44. The superscripts, *, ** and *** denote a significant increase (*, P<0.05; **P<0.01, ***P<0.001) compared with unstimulated cells (NT). # denotes a significant decrease (P<0.01) for the stimulation by trypsin (10 nM) in the presence of the Rho-Kinase inhibitor, Y27362 (10 μM), compared with cells stimulated by trypsin in the absence of the inhibitor. Data are representative of three independent experiments.

Figure 7: Over expression of Gα12 and Gα13 increases sensitivity to trypsin for MAPK activation in rPAR$_2$-L^{37}S^{38} transfected KNRK cells. (A) Representative western blots visualizing activated (top gel: phospho(P)-p42/44) and total enzyme (lower gel: total(T)-p42/44) in control cells or cells transiently over expressing Gα12 and Gα13 and activated with 5 or 10nM trypsin. **(B)** Quantitative densitometric image analysis of MAPkinase activation expressed as the percentage increase over basal levels of phospho(P)-p42/44 normalized to total(T)p42/44 in response to activation with 5 or 10nM

Molecular Pharmacology Fast Forward. Published on July 15, 2009 as DOI: 10.1124/mol.109.055509
This article has not been copyedited and formatted. The final version may differ from this version.

trypsin. * indicates a significant increase over basal levels ($P<0.05$). Data are representative of two independently conducted experiments.

Figure 8: Trypsin stimulates MAPkinase signaling in β-arrestin null DKO MEF cells transfected with (A) wt-rPAR$_2$, (B) rPAR$_2$-L^{37}S^{38} or (C) rPAR$_2$-A$^{37-38}$ MAPkinase activation, expressed as a fold-increase (phospho(P)-p42/44) relative to total enzyme (T-p42/44), as monitored at timed intervals for receptors expressed in either wild-type fibroblasts (○: MEF wt) or β-arrestin null fibroblasts (■, MEF DKO). Data points, showing the average values for triplicate measurements (± s.e.m., Bars), are representative of three independent experiments.

Figure 9: BRET measurements show a lack of trypsin-stimulated recruitment of β arrestin-2 to rPAR$_2$-L^{37}S^{38} (C) and rPAR$_2$-A$^{37-38}$ (D), compared with trypsin-stimulated wt-rPAR$_2$ (A) and SLIGRL-NH$_2$-activated receptors (A and insets, Panels C and D). BRET measurements (BRET rLUC/YFP) were done as described in Materials and Methods to monitor recruitment of β arrestin-2 to wt-rPAR$_2$ **(A and B),** rPAR$_2$-L^{37}S^{38} **(C)** and rPAR$_2$-A$^{37-38}$ **(D)**. As outlined in Materials and Methods, HEK cells transiently expressing the receptors were activated either by trypsin (panels A, C and D) or by the PAR2-activating peptide (panel B and insets, panels C and D) and the BRET signals (light and dark tracings) reflecting a receptor-β arrestin-2 interaction were monitored continuously (seconds) over a 20 min time period. An agonist-mediated increase in the BRET signal (agonist-stimulated dark tracings, panels A, B and insets, panels C and D) relative to baseline (light tracings) indicates a recruitment of β arrestin-2 to the activated receptor. No increased BRET was observed for trypsin-treated TL-mutant receptors (coincidence of dark and light tracings, Panels C and D). Data are representative of three independently conducted experiments.

Molecular Pharmacology Fast Forward. Published on July 15, 2009 as DOI: 10.1124/mol.109.055509
This article has not been copyedited and formatted. The final version may differ from this version.

Figure 10: Lack of internalization of trypsin-activated rPAR$_2$-L^{37}S^{38} (Panel v) and rPAR$_2$-A$^{37-38}$ (Panel viii), compared with wt-rPAR$_2$ (Panel ii) and with SLIGRL-NH$_2$-activated receptors (Panels iii, vi, ix). Transiently transfected receptor-expressing HEK cells, either untreated (NT: panels i, iv and vii) or treated for 30 min at 37º C with either trypsin (Panels ii, v and vii) or SLIGRL-NH$_2$ (Panels iii and insets, Panels vi and ix) were then fixed (4% formalin, 5 min) to enable visualization of the YFP-tagged receptors, as outlined in Methods and Materials. **UPPER PANELS:** (A) Representative images for wt-rPAR$_2$ (i to iii), rPAR$_2$-L^{37}S^{38} (iv to vi) and rPAR$_2$-A$^{37-38}$ (vii to ix). **LOWER HISTOGRAMS:** (B) Quantitative morphometric analysis of receptor internalization done as outlined in Materials and Methods for either untreated cells (NT, open histograms) or following treatment with either trypsin (grey histograms) or SLIGRL-NH$_2$ (filled histograms). Internalization, measured in three independently conducted experiments, is expressed as the average number of internalized fluorescent speckles per cell (± s.e.m., Bars). The superscript, *, denotes a significantly reduced ($P<0.01$) trypsin-activated internalization in the TL-mutant receptor-expressing cells compared with cells expressing the wild-type receptor.

Figure 11: Selective activation of p42/44 MAPkinase in PAR$_2$ transfected KNRK cells by SLAAAA-NH$_2$ compared with the TL-mutant-derived synthetic peptides, AAIGRL-NH2 and LSIGRL-NH$_2$. KNRK cell lines expressing wt-rPAR$_2$, rPAR$_2$-L^{37}S^{38} and rPAR$_2$-A$^{37-38}$ were treated for 10 min at 37º C with the synthetic PAR$_2$ tethered ligand-related peptides, SLAAAA-NH$_2$, LSIGRL-NH$_2$ and AAIGRL-NH$_2$ or with trypsin and the activation of MAPkinase was monitored (phospho(P)-p42/44) relative to total(T)-p42/44) by western blot analysis as outlined by the legend to Fig. 2. **(A)** representative western blot detection of the activation of MAPkinase (phospho(P)-42/44, relative to total(T)-p42/44) in wt-rPAR$_2$ by SLAAAA-NH$_2$ (third lane from left) but not by LSIGRL-NH$_2$ and AAIGRL-NH$_2$ (second and fourth lanes from left). **(B)** Representative western blots for the activation

Molecular Pharmacology Fast Forward. Published on July 15, 2009 as DOI: 10.1124/mol.109.055509
This article has not been copyedited and formatted. The final version may differ from this version.

of MAPkinase (phospho(P)-p42/44, relative to total(T)-p42/44) in wt-rPAR$_2$, (upper), rPAR$_2$-L^{37}S^{38} (middle) and rPAR$_2$-A$^{37\text{-}38}$ (lower) by trypsin (10 nM), SLIGRL-NH$_2$ (10 μM) or SLAAAA-NH$_2$ (10 μM). **(C)** Quantitative densitometric image analysis for the percentage increase over baseline (no treatment: NT) of phospho(P)-p42/44, normalized to total(T)-p42/44, as shown in panel B, for activation of wt-rPAR$_2$ (solid histograms), rPAR$_2$-L^{37}S^{38} (open histograms) and rPAR$_2$-A$^{37\text{-}38}$ (grey histograms). The quantitative densitometry values (histograms) are expressed as averages (± s.e.m., Bars) for three or more independently conducted experiments.

Molecular Pharmacology Fast Forward. Published on July 15, 2009 as DOI: 10.1124/mol.109.055509
This article has not been copyedited and formatted. The final version may differ from this version.

Clone	Cleavage Activation site	TL derived peptide
wt-$rPAR_2$	R/SLIGRL….	SLIGRL-NH_2
$rPAR_2$-$L^{37}S^{38}$	R/LSIGRL….	LSIGRL-NH_2
$rPAR_2$-A^{37-38}	R/AAIGRL….	AAIGRL-NH_2

Table 1: wt-$rPAR_2$ and tethered ligand mutated $rPAR_2$ variants showing the cleavage-activation sequences resulting from trypsin exposure and the corresponding synthetic agonist peptides.

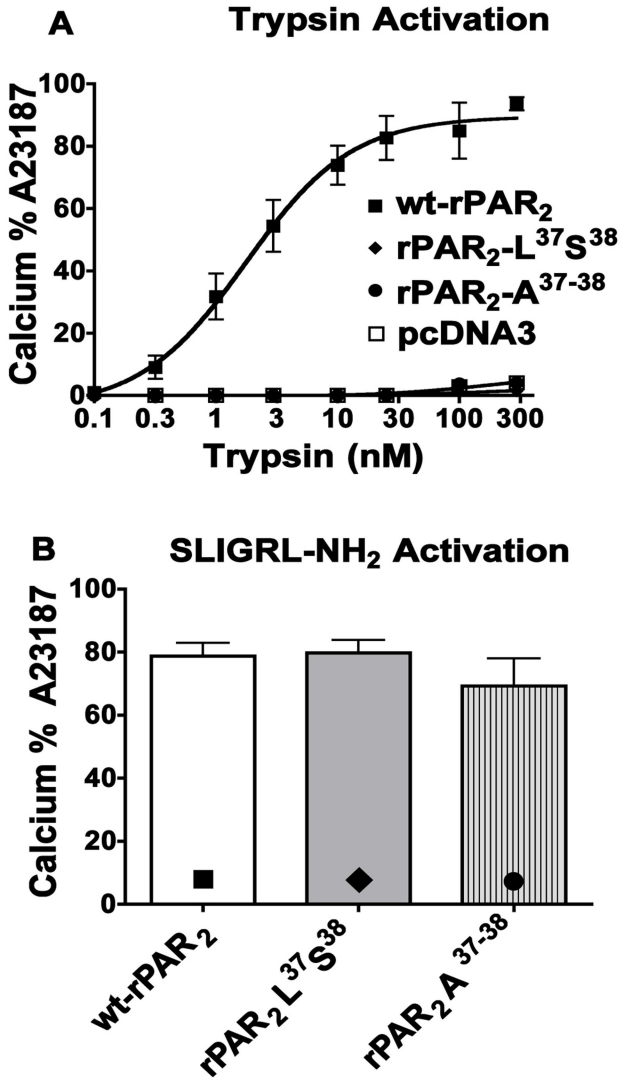

Figure 1

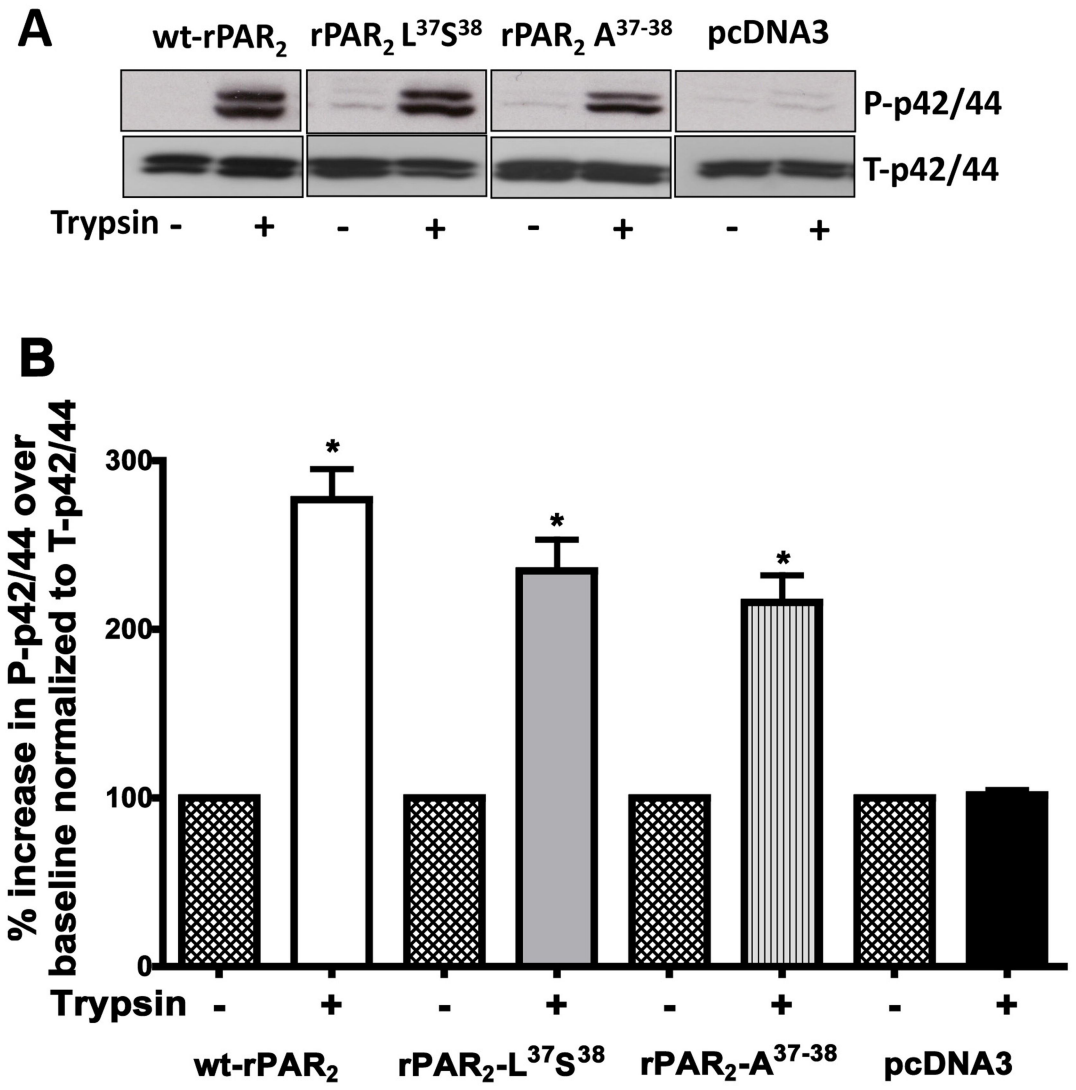

Figure 2

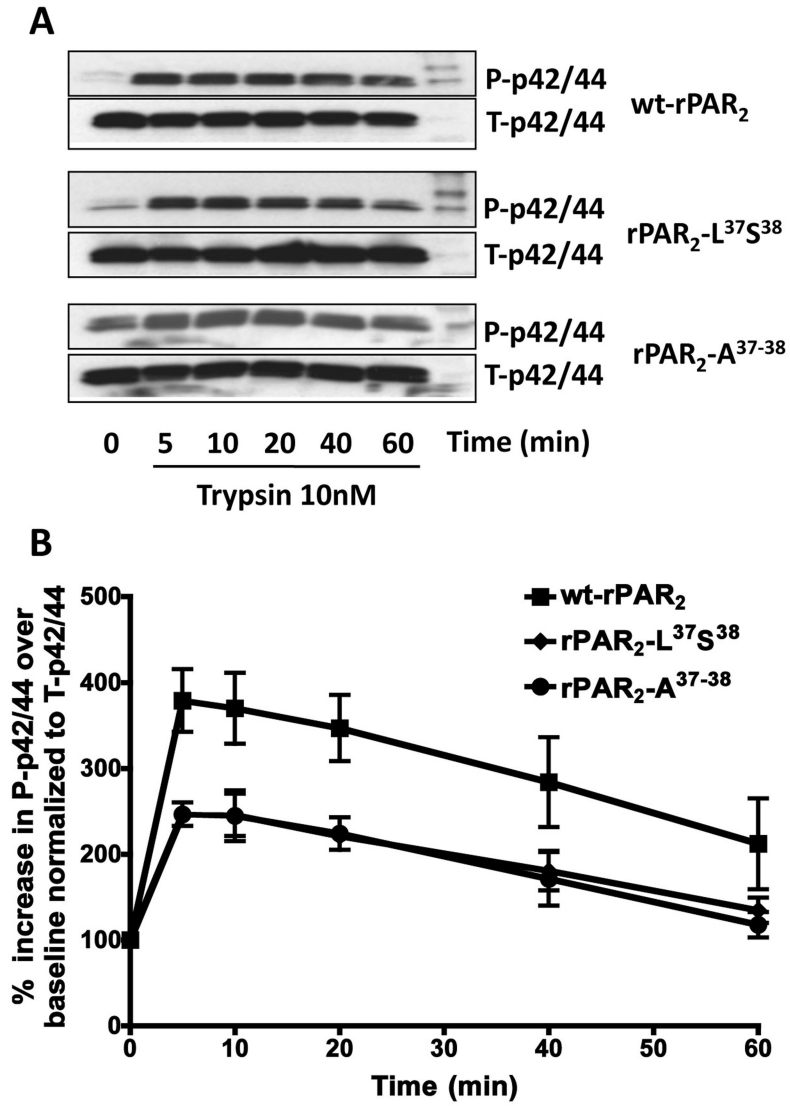

Figure 3

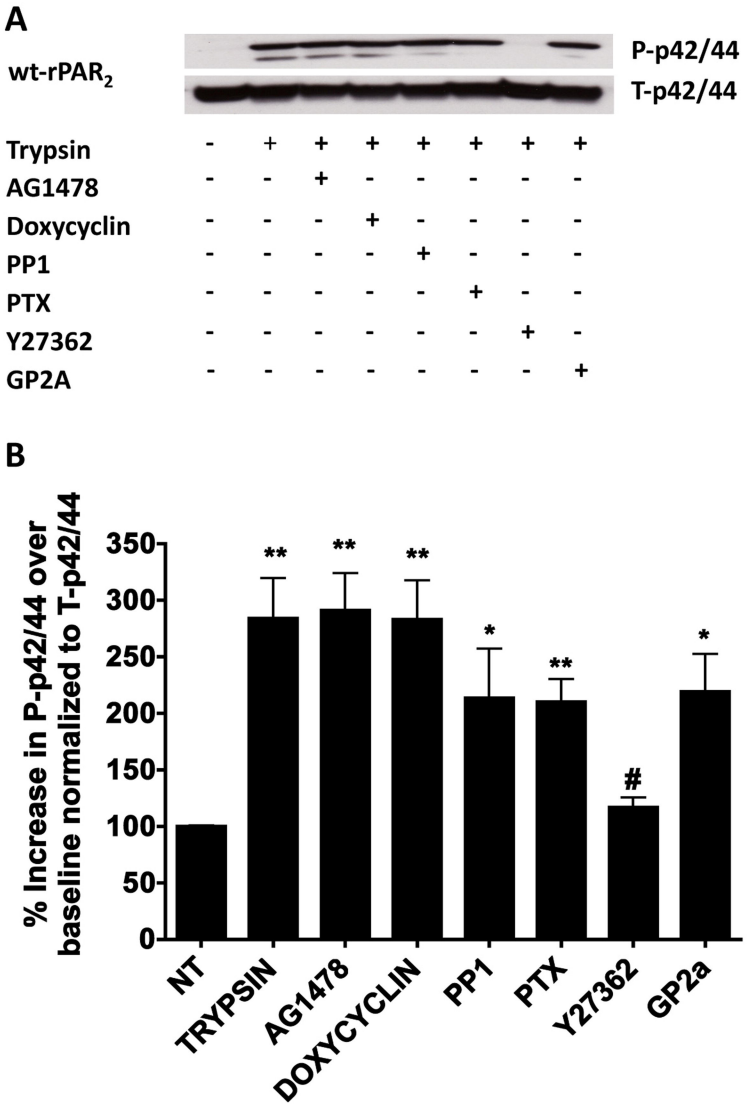

Figure 4

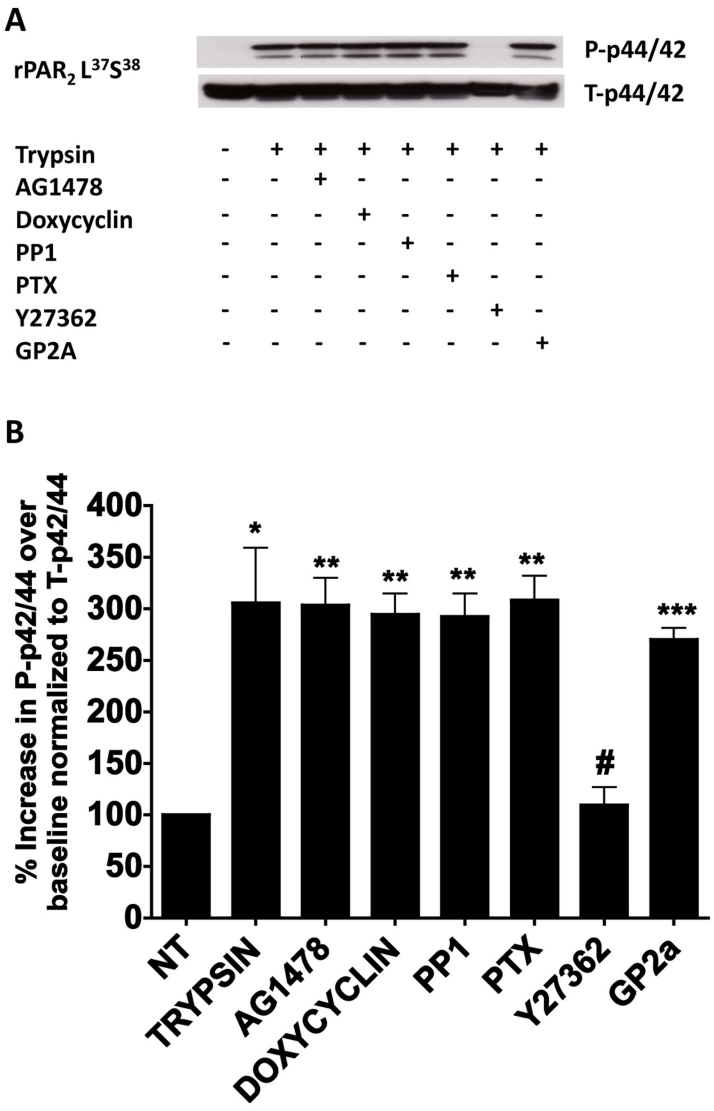

Figure 5

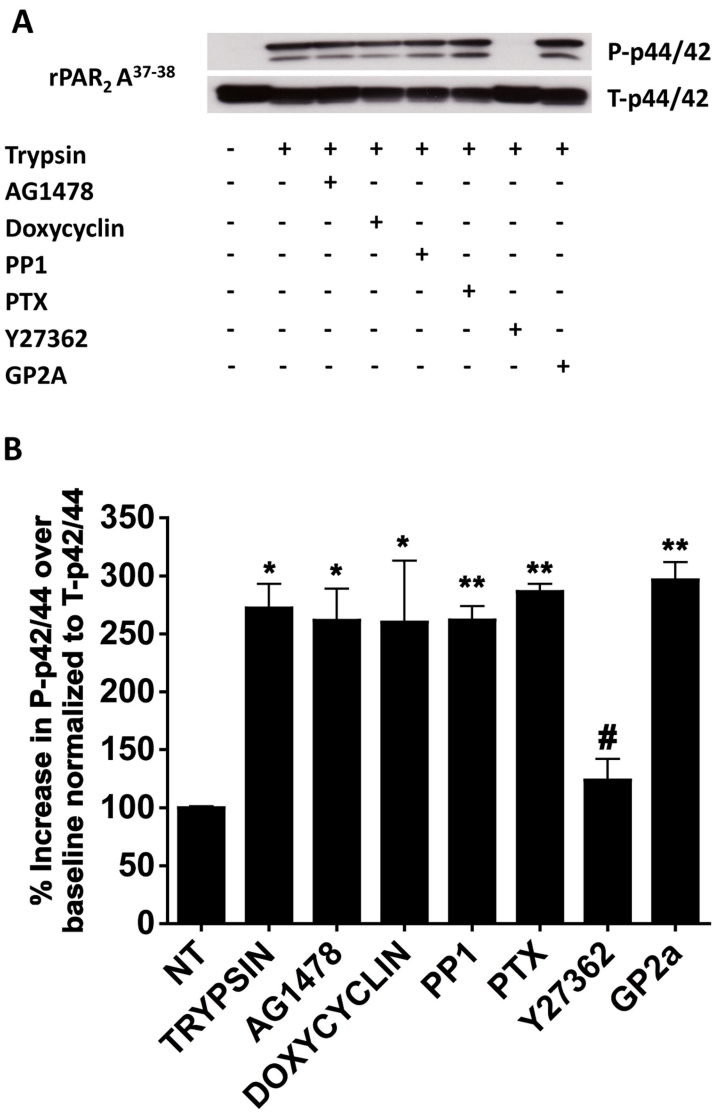

Figure 6

Molecular Pharmacology Fast Forward. Published on July 15, 2009 as DOI: 10.1124/mol.109.055509
This article has not been copyedited and formatted. The final version may differ from this version.

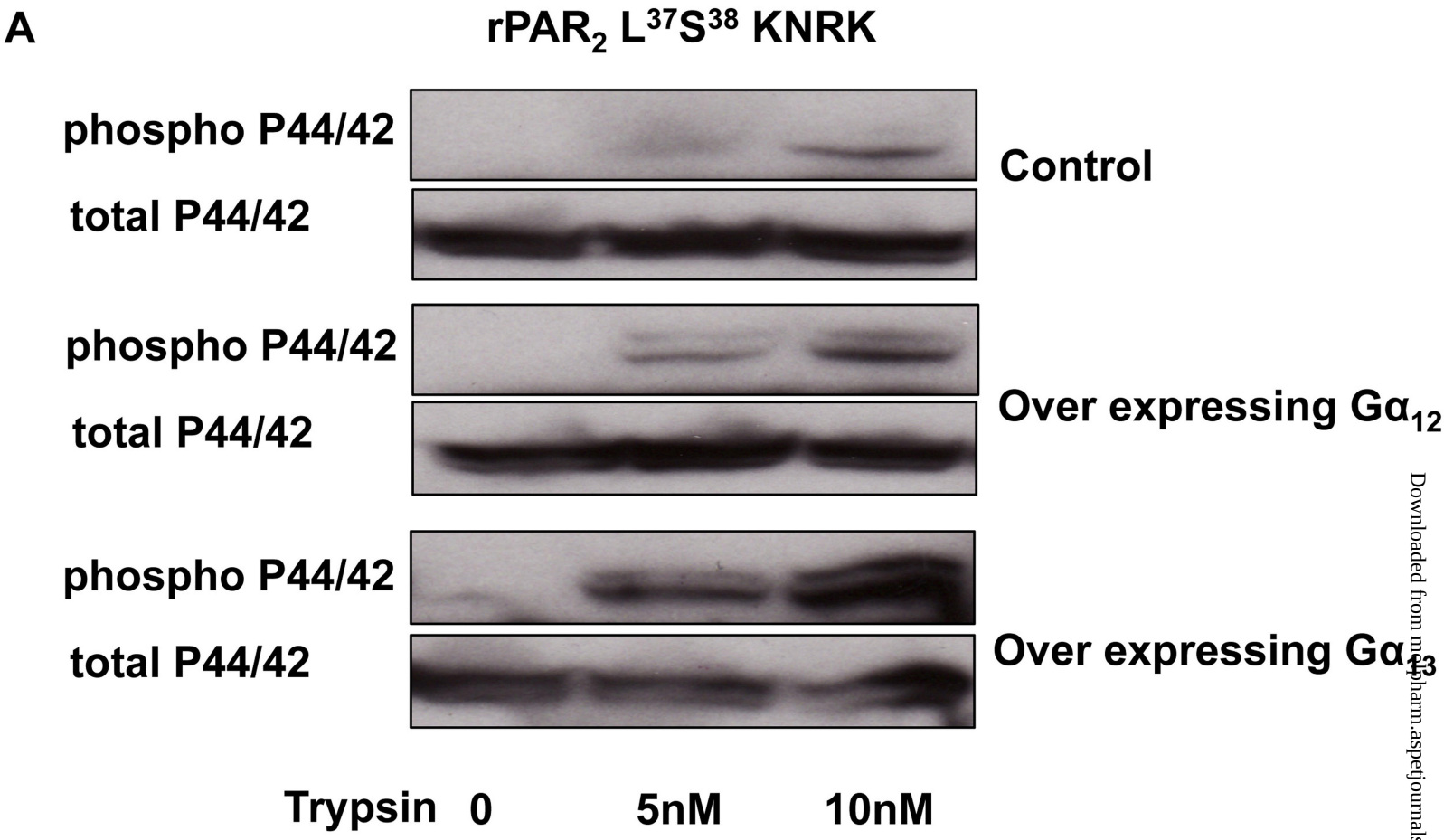

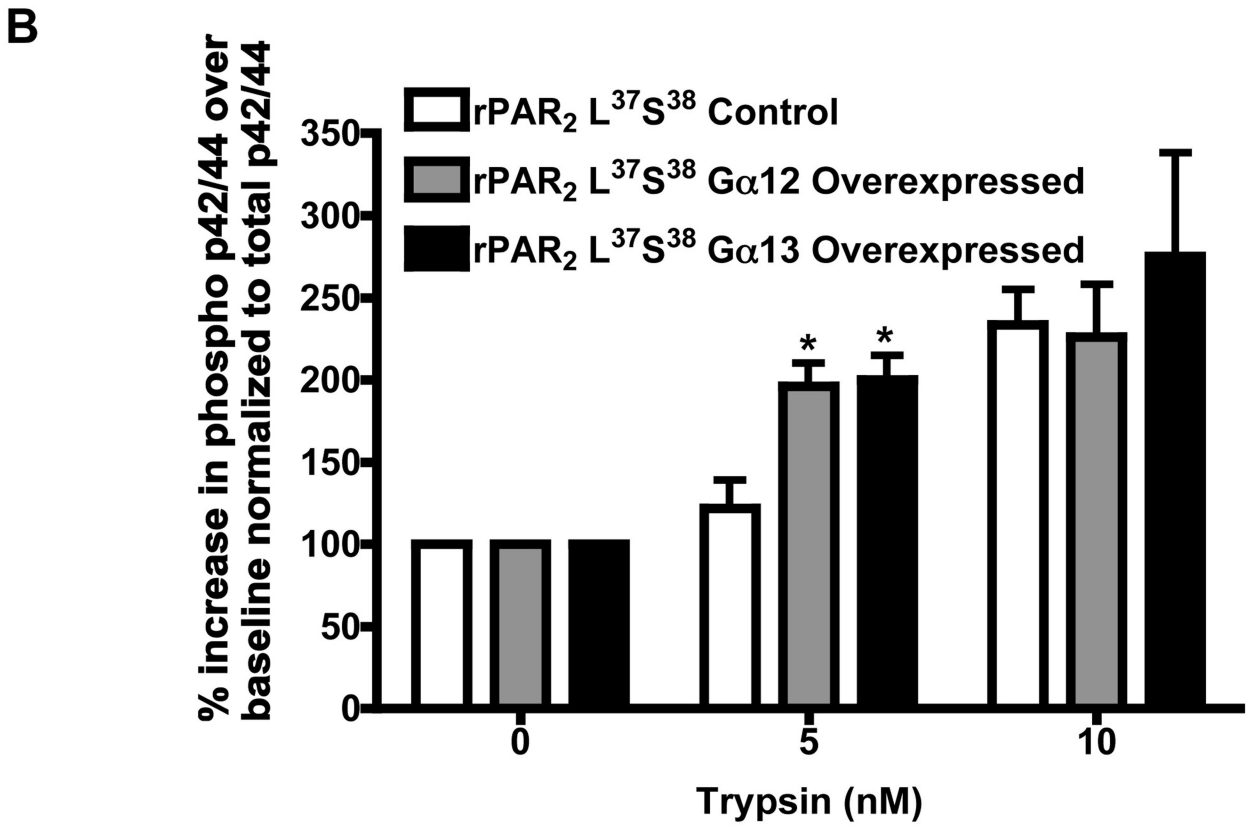

Figure 7

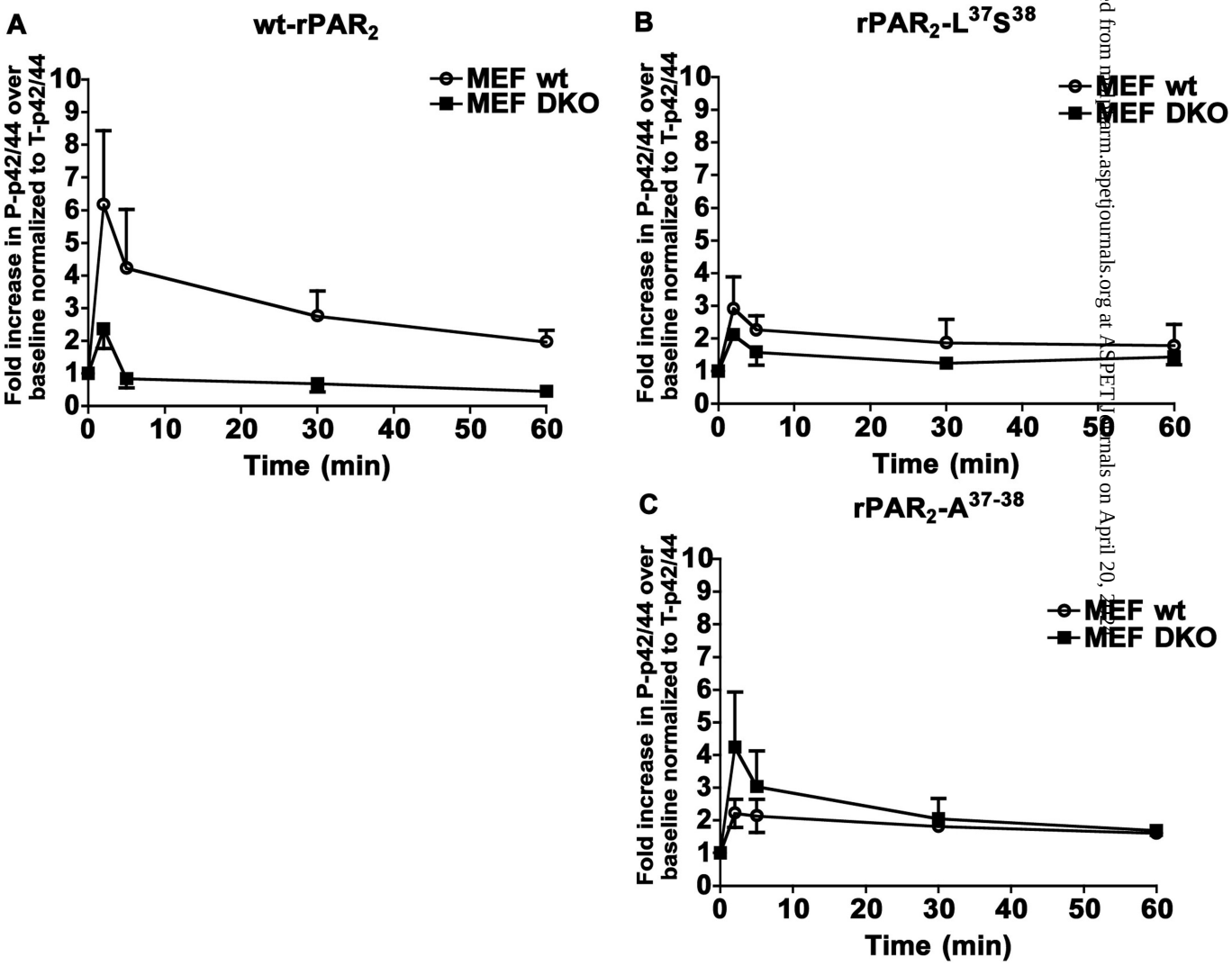

Figure 8

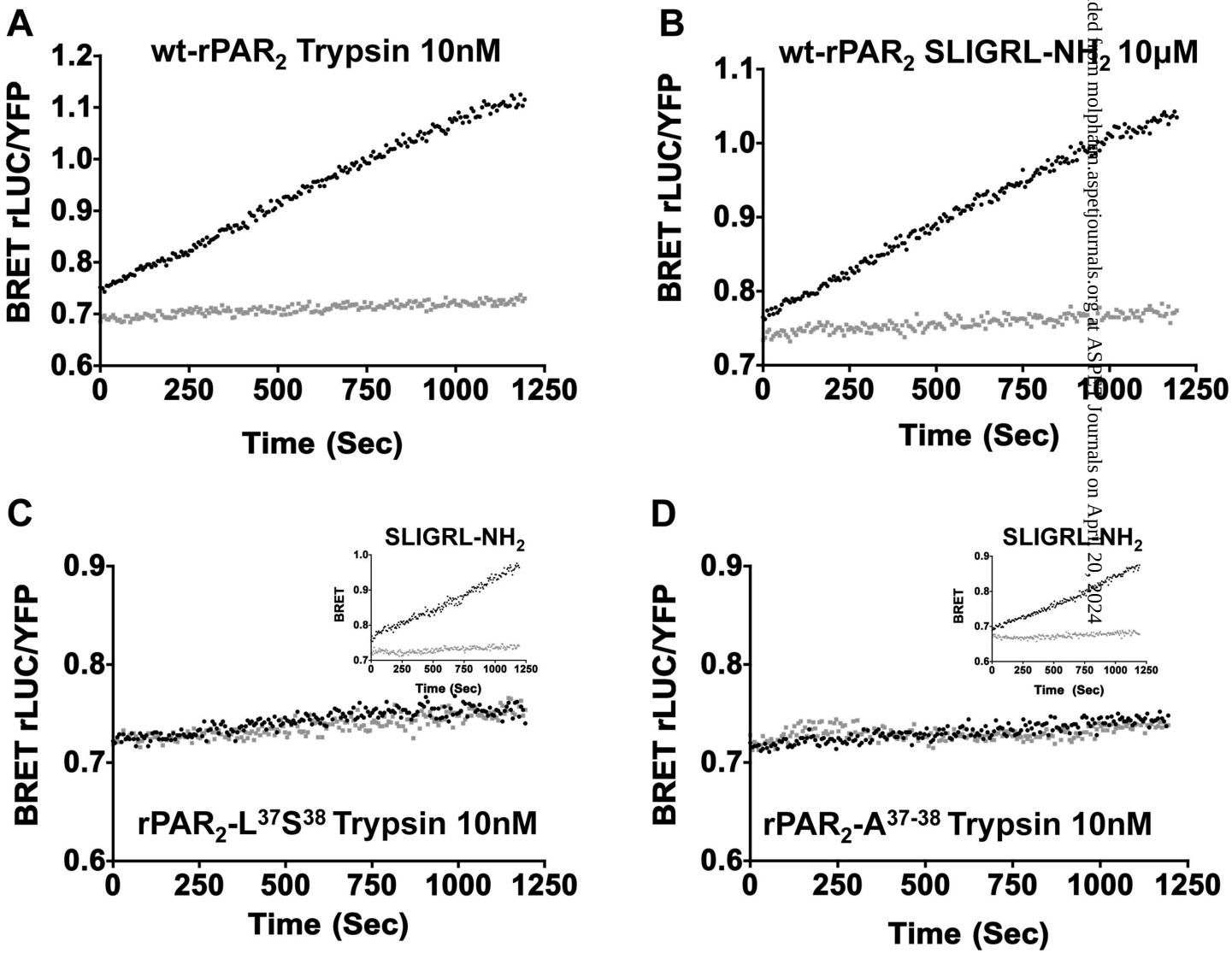

Figure 9

Molecular Pharmacology Fast Forward. Published on July 15, 2009 as DOI: 10.1124/mol.109.055509
This article has not been copyedited and formatted. The final version may differ from this version.

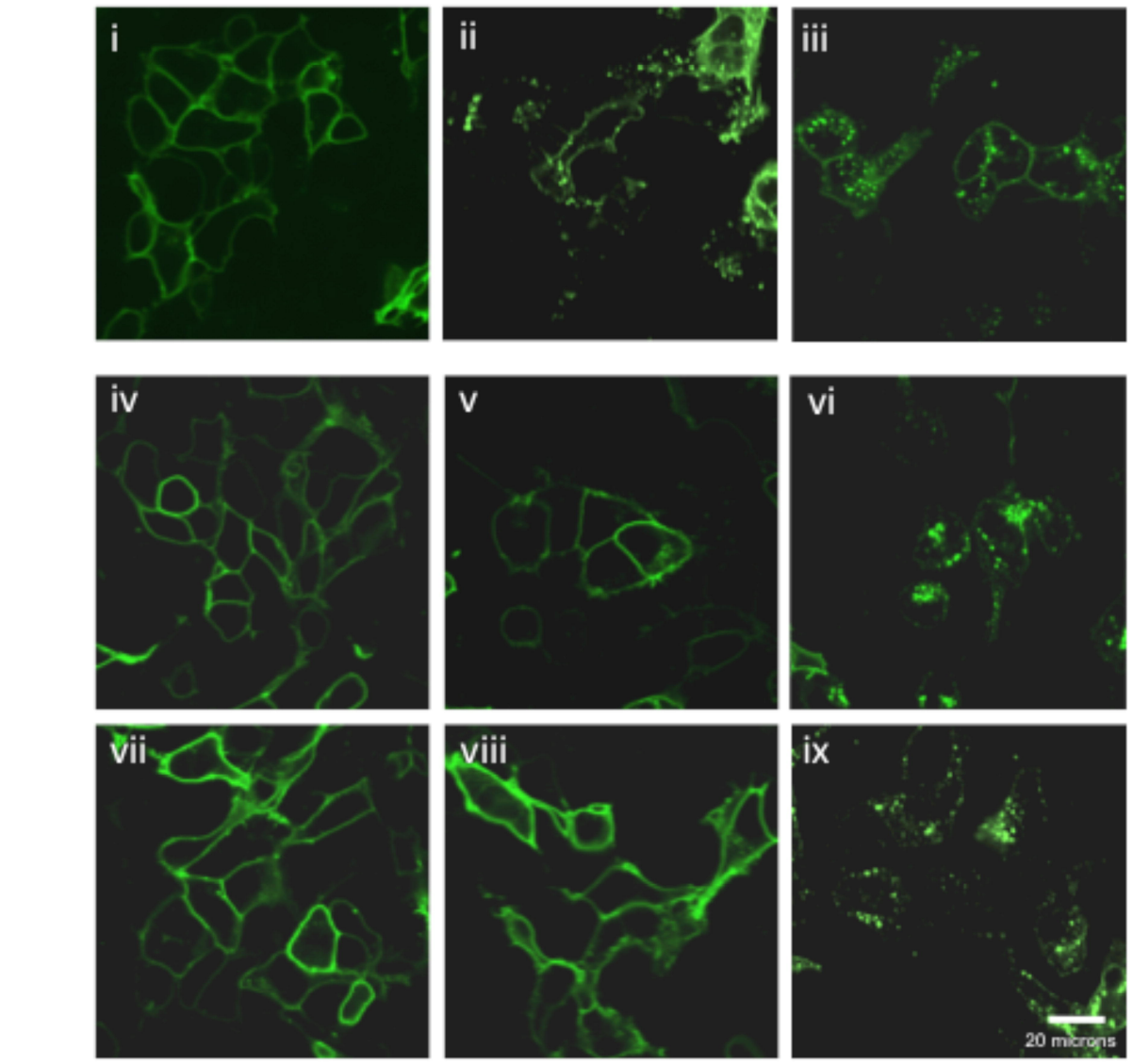

Figure 10

A

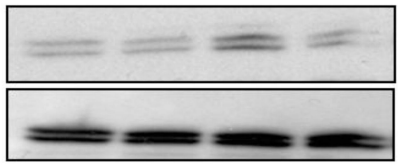

LSIGRL-NH_2 10µM - + - -

SLAAAA-NH_2 10µM - - + -

AAIGRL-NH_2 10µM - - - +

B

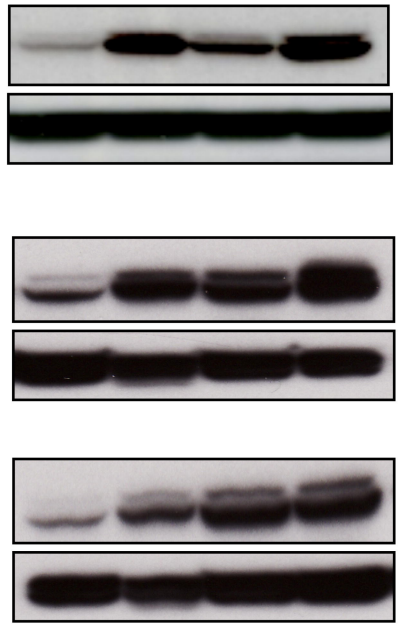

Trypsin 10nM - + - -

SLIGRL-NH_2 10µM - - + -

SLAAAA-NH_2 10µM - - - +

C

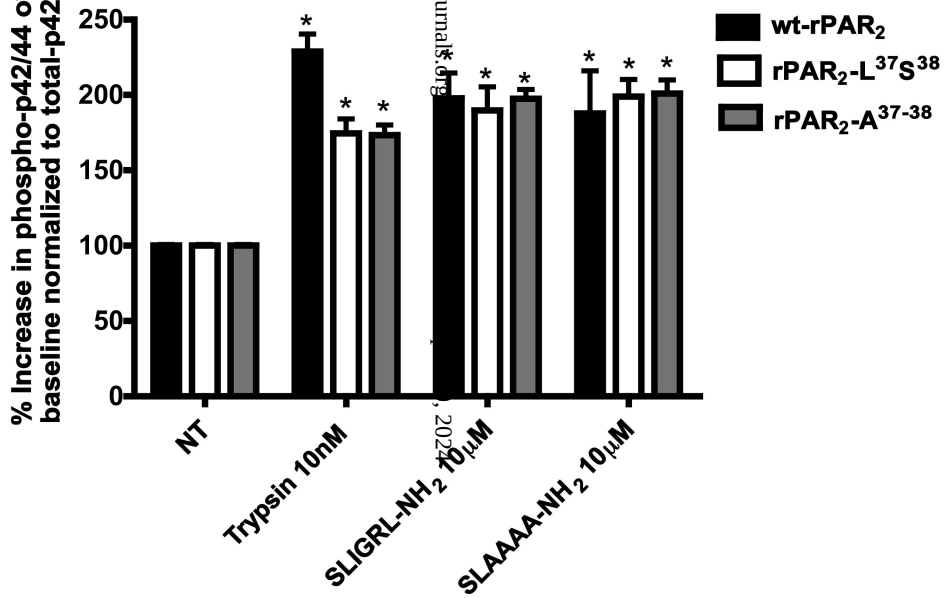

Figure 11